



Universiteit
Leiden
The Netherlands

Kinetic profiling and functional characterization of 8-phenylxanthine derivatives as A2B adenosine receptor antagonists

Vlachodimou, A.; Vries, H. de; Pasoli, M.; Goudswaard, M.; Kim, S.A.; Kim, Y.C.; ... ; IJzerman, A.P.

Citation

Vlachodimou, A., Vries, H. de, Pasoli, M., Goudswaard, M., Kim, S. A., Kim, Y. C., ... IJzerman, A. P. (2022). Kinetic profiling and functional characterization of 8-phenylxanthine derivatives as A2B adenosine receptor antagonists. *Biochemical Pharmacology*, 200. doi:10.1016/j.bcp.2022.115027

Version: Publisher's Version

License: [Creative Commons CC BY 4.0 license](https://creativecommons.org/licenses/by/4.0/)

Downloaded from: <https://hdl.handle.net/1887/3420598>

Note: To cite this publication please use the final published version (if applicable).



Kinetic profiling and functional characterization of 8-phenylxanthine derivatives as A_{2B} adenosine receptor antagonists

Anna Vlachodimou^a, Henk de Vries^a, Milena Pasoli^a, Miranda Goudswaard^a, Soon-Ai Kim^b, Yong-Chul Kim^b, Mirko Scortichini^b, Melissa Marshall^d, Joel Linden^d, Laura H. Heitman^{a,c}, Kenneth A. Jacobson^{b,*}, Adriaan P. IJzerman^{a,*}

^a Division of Drug Discovery and Safety, Leiden Academic Centre for Drug Research (LACDR), Leiden University, P.O. Box 9502, 2300 RA Leiden, the Netherlands

^b Laboratory of Bioorganic Chemistry, National Institute of Diabetes and Digestive and Kidney Diseases, NIH, 9000 Rockville Pike, Bethesda, MD 20892, USA

^c Oncode Institute, Leiden, the Netherlands

^d Department of Internal Medicine and Molecular Physiology & Biological Physics, University of Virginia Health Science Center, Charlottesville, VA 22908, USA

ARTICLE INFO

Keywords:

A_{2B} adenosine receptor
Antagonists
Binding kinetics
Radioligand binding assay
Label-free functional assay
Covalent binding

ABSTRACT

A_{2B} adenosine receptor (A_{2B}AR) antagonists have therapeutic potential in inflammation-related diseases such as asthma, chronic obstructive pulmonary disease and cancer. However, no drug is currently clinically approved, creating a demand for research on novel antagonists. Over the last decade, the study of target binding kinetics, along with affinity and potency, has been proven valuable in early drug discovery stages, as it is associated with improved *in vivo* drug efficacy and safety. In this study, we report the synthesis and biological evaluation of a series of xanthine derivatives as A_{2B}AR antagonists, including an isothiocyanate derivative designed to bind covalently to the receptor. All 28 final compounds were assessed in radioligand binding experiments, to evaluate their affinity and for those qualifying, kinetic binding parameters. Both structure-affinity and structure-kinetic relationships were derived, providing a clear relationship between affinity and dissociation rate constants. Two structurally similar compounds, **17** and **18**, were further evaluated in a label-free assay due to their divergent kinetic profiles. An extended cellular response was associated with long A_{2B}AR residence times. This link between a ligand's A_{2B}AR residence time and its functional effect highlights the importance of binding kinetics as a selection parameter in the early stages of drug discovery.

1. Introduction

The A_{2B} adenosine receptor (A_{2B}AR) belongs to the superfamily of rhodopsin-like G protein-coupled receptors (GPCRs), being a member of the adenosine receptor (AR) family. It has been mapped on chromosome 17p11.2-12, and as all GPCRs the encoded protein consists of a seven transmembrane (7TM) α -helix architecture [1,2]. Adenosine, a ubiquitous purine nucleoside, is the endogenous ligand for all ARs, i.e. A₁, A_{2A}, A_{2B} and A₃. These AR subtypes are coupled to different effectors and modulate different physiological and pathophysiological conditions. A_{2B}AR is the least well characterized of the four AR subtypes, possibly

due to its low affinity for adenosine [3]. Under physiological conditions A_{2B}AR is considered to remain silent, as the extracellular concentration of adenosine ranges from 20 to 300 nM, much lower than the reported half maximal effective concentration (EC₅₀) of adenosine for A_{2B}AR (EC₅₀ = 24 μ M). In contrast, under pathophysiological conditions extracellular concentrations of adenosine could rise up to 30 μ M, therefore resulting in A_{2B}AR activation and signaling [4,5].

A_{2B}ARs are present in numerous tissues and organs, including bowel, bladder, lung, brain, as well as on hematopoietic and mast cells [2,6]. Interestingly, A_{2B}AR expression levels are often (up)regulated during disease. The high expression of the receptor in conjunction with the

Abbreviations: AR, adenosine receptor; BCA, bicinchoninic acid; BSA, bovine serum albumin; CGS21680, 4-[2-[[6-amino-9-(N-ethyl- β -D-ribofuranuronamidoyl)-9H-purin-2-yl]amino]ethyl]benzenepropanoic acid; CHAPS, 3-[(3-cholamidopropyl)dimethylammonio]-1-propanesulfonate hydrate; cmpd, compound; DMSO, dimethyl sulfoxide; GPCR, G protein-coupled receptor; h, human; I-AB-MECA, 3-iodo-4-aminobenzyl-5'-N-methylcarboxamidoadenosine; I-ABOPX, 2-[4-[3-[(4-amino-3-iodophenyl)methyl]-2,6-dioxo-1-propyl-7H-purin-8-yl]phenoxy]acetic acid; NECA, 5'-N-ethylcarboxamidoadenosine; NSB, non-specific binding; R-PIA, N⁶-R-phenylisopropyladenosine; RT, residence time; SAR, structure-affinity relationship; SKR, structure-kinetics relationship; TB, total binding.

* Corresponding authors.

E-mail addresses: kennethj@nidk.nih.gov (K.A. Jacobson), ijzerman@lacdr.leidenuniv.nl (A.P. IJzerman).

<https://doi.org/10.1016/j.bcp.2022.115027>

Received 10 February 2022; Received in revised form 22 March 2022; Accepted 24 March 2022

Available online 6 April 2022

0006-2952/© 2022 The Author(s). Published by Elsevier Inc. This is an open access article under the CC BY license (<http://creativecommons.org/licenses/by/4.0/>).

increased extracellular adenosine concentration under pathophysiological conditions render $A_{2B}AR$ antagonists interesting pharmacological and therapeutic tools for a broad spectrum of diseases, such as asthma, chronic obstructive pulmonary disease [7,8], colon inflammation [9,10], diabetes [11] and cancer [12]. Adenosine production is upregulated in the tumor microenvironment and acts at both $A_{2A}AR$ and $A_{2B}AR$ to facilitate tumor progression *in vivo* [13]. In cancer models $A_{2B}AR$ antagonists impede adenosine-induced tumor cell proliferation, angiogenesis and metastasis, and remove immune suppression [14].

Over the past years, various xanthine and non-xanthine derivatives have been synthesized and evaluated for their $A_{2B}AR$ affinity and selectivity [15–18]. However, no $A_{2B}AR$ -selective antagonist has reached the market yet for therapeutic use. Only CVT-6883 has completed Phase I clinical trials with no adverse events reported, while another clinical trial for PBF-1129, as drug candidate for locally advanced or metastatic non-small cell lung carcinoma, is under recruitment [19,20].

The 3D structure of $A_{2B}AR$ has not been elucidated yet, hence, the design of new potential drug candidates is mainly based on more classical structure-affinity relationships or on molecular modeling based on homology to the $A_{2A}AR$ [21]. Although affinity is a key parameter in pharmacology, it does not necessarily predict *in vivo* efficacy. During the last decade an increasing number of studies suggested that the study of ligand binding kinetics, quantified by association (k_{on}) and dissociation (k_{off}) rate constants, is highly relevant in the early stages of drug discovery, as *in vivo* efficacy is linked to optimized kinetic characteristics in many cases [22]. A typical example is the neurokinin 1 (NK_1) receptor antagonist aprepitant, an antiemetic. Aprepitant has been found to have higher *in vivo* efficacy than other NK_1 receptor antagonists with similar thermodynamic affinities, due to its long residence time (RT: $1/k_{off}$) at the NK_1 receptor [23].

Here, we report on the synthesis of a number of xanthine-based $A_{2B}AR$ antagonists, on the affinities of these and a number of previously reported xanthines, and on their kinetic target binding parameters obtained in radioligand binding assays. Although not very selective most xanthine derivatives present high affinity for $A_{2B}AR$, while displaying a variety in association and dissociation rate constants. On the basis of these results we also synthesized and pharmacologically profiled compound **29**, a xanthine antagonist that presumably binds covalently to $A_{2B}AR$. Additionally, we developed a label-free impedance-based assay using intact cells expressing $A_{2B}AR$ for the further characterization of compounds with diverse kinetic profiles. Compounds **17** and **18** with a long and short RT on the receptor, respectively, were profiled in this assay. Compound **17**, with the longer RT, had a more sustained effect than compound **18**, suggesting this assay has translational relevance.

2. Materials and methods

2.1. Chemistry

Synthetic reagents and solvents were purchased from Sigma-Aldrich (St. Louis, MO, USA), or prepared as reported. 1H NMR spectra were obtained with a Bruker 400 spectrometer using $CDCl_3$, $DMSO-d_6$, acetone- d_6 or $CDCl_3$ as a solvent. The chemical shifts are expressed as ppm, and the coupling constants (J) are given in Hz. High resolution mass (HRMS) measurements were performed on a proteomics optimized Micromass Q-TOF-2 (Waters, Milford, MA, USA). All chemicals not further specified were from standard commercial sources. Compounds **2**, **8**, **11–19**, **26** and **27** were reported in Kim *et al.* [24].

2.1.1. General procedure for the preparation of benzylamide derivatives **3–7**, **9**, **10**, **20–25**, and **28**

A solution of XCC (**1**), 8-[4-[carboxymethoxy]phenyl]-1,3-di-(*n*-propyl)xanthine (1 eq) [25], the desired amine compound (1 eq), EDAC (1-ethyl-3-(2-dimethylaminoethyl)carbodiimide, 2 eq.) and DMAP (4-[*N,N*-(dimethylamino)]pyridine, 2.2 eq) in 2 mL of anhydrous

dimethylformamide was stirred at room temperature for 24 h. The reaction mixture was evaporated to dryness under a stream of nitrogen, and the residue was purified by preparative silica gel thin layer chromatography (chloroform:methanol = 20:1) and crystallization in methanol/ethyl ether to afford the desired compounds.

N-cyclopropyl-2-(4-(2,6-dioxo-1,3-dipropyl-2,3,6,7-tetrahydro-1H-purin-8-yl)phenoxy)acetamide (3). Compound **3** was synthesized following the general procedure using cyclopropylamine and obtaining 15.0 mg of pure compound (68% yield).

1H NMR ($DMSO$, 400 Hz) δ 8.17 (d, 1H, $J = 3.3$ Hz), 8.06 (d, 2H, $J = 8.7$ Hz), 7.06 (d, 2H, $J = 8.7$ Hz, 2H), 4.51 (s, 2H), 4.01 (t, 2H, $J = 7.1$ Hz), 3.86 (t, 2H, $J = 7.3$ Hz), 3.87 (t, 2H, $J = 7.3$ Hz), 2.67–2.71 (m, 1H), 1.73 (q, 2H, $J = 7.4$, 14.5 Hz), 1.57 (q, 2H, $J = 7.4$, 14.5 Hz), 0.85–0.92 (m, 6H), 0.61–0.66 (m, 2H), 0.46–0.50 (m, 2H).

HRMS calcd $C_{22}H_{28}N_5O_4$ ($M + H$) $^+$: 426.2141; found 426.2139.

N-cyclobutyl-2-(4-(2,6-dioxo-1,3-dipropyl-2,3,6,7-tetrahydro-1H-purin-8-yl)phenoxy)acetamide (4). Compound **4** was synthesized following the general procedure using cyclobutylamine and obtaining 19.0 mg of pure compound (95% yield).

1H NMR ($DMSO + CDCl_3$, 300 Hz) δ 8.26 (d, 1H, $J = 8.1$ Hz), 8.60 (d, 2H, $J = 9.0$ Hz), 7.59 (d, 2H, $J = 9.0$ Hz), 4.49 (s, 2H), 4.28 (dd, 1H, $J = 7.5$, 16.2 Hz), 4.20 (t, 2H, $J = 7.2$ Hz), 3.88 (t, 2H, $J = 7.4$ Hz), 2.1–2.2 (m, 2H), 1.94–2.4 (m, 2H), 1.71–1.80 (m, 2H), 1.54–1.71 (m, 4H), 0.92 (t, 3H, $J = 5.1$ Hz), 0.87 (t, 3H, $J = 5.1$ Hz).

HRMS calcd $C_{24}H_{23}N_6O_4$ ($M + H$) $^+$: 459.1781; found 459.1779.

N-cyclopentyl-2-(4-(2,6-dioxo-1,3-dipropyl-2,3,6,7-tetrahydro-1H-purin-8-yl)phenoxy)acetamide (5). Compound **5** was synthesized following the general procedure using cyclopentylamine and obtaining 20.0 mg of pure compound (85% yield).

1H NMR ($DMSO$, 400 Hz) δ 8.06 (d, 2H, $J = 8.7$ Hz), 8.01 (d, 1H, $J = 5.3$ Hz), 7.06 (d, 2H, $J = 8.8$ Hz, 2H), 4.52 (s, 2H), 3.99–4.08 (m, 4H), 3.84 (t, 4H, $J = 7.4$ Hz), 1.40–1.82 (m, 12H), 0.85–0.92 (m, 6H).

HRMS calcd $C_{24}H_{32}N_5O_4$ ($M + H$) $^+$: 454.2454; found 454.2457.

2-(4-(2,6-dioxo-1,3-dipropyl-2,3,6,7-tetrahydro-1H-purin-8-yl)phenoxy)-N-(1H-pyrazol-3-yl)acetamide (6). Compound **6** was synthesized following the general procedure using 3-aminopyrazole and obtaining 5.0 mg of pure compound (21% yield).

1H NMR ($DMSO$, 400 Hz) δ 12.39 (s, 1H), 10.56 (s, 1H), 8.07 (d, 2H, $J = 8.7$ Hz), 7.62 (s, 1H), 7.09 (d, 2H, $J = 8.6$ Hz, 2H), 6.49 (s, 1H), 4.77 (s, 2H), 4.01 (s, 2H), 3.86 (t, 2H, $J = 7.2$ Hz), 1.72 (q, 2H, $J = 7.4$, 14.5 Hz), 1.57 (q, 2H, $J = 7.3$, 14.4 Hz), 0.85–0.92 (m, 6H).

HRMS calcd $C_{22}H_{26}N_7O_4$ ($M + H$) $^+$: 452.2046; found 452.2047.

N-cyclohexyl-2-(4-(2,6-dioxo-1,3-dipropyl-2,3,6,7-tetrahydro-1H-purin-8-yl)phenoxy)acetamide (7). Compound **7** was synthesized following the general procedure using cyclohexylamine and obtaining 19.0 mg of pure compound (79% yield).

1H NMR ($DMSO$, 400 Hz) δ 8.06 (d, 2H, $J = 8.7$ Hz), 7.92 (d, 1H, $J = 8.2$ Hz), 7.07 (d, 2H, $J = 8.7$ Hz, 2H), 4.52 (s, 2H), 4.01 (t, 2H, $J = 7.2$ Hz), 3.86 (t, 2H, $J = 7.3$ Hz), 3.61 (s, 1H), 1.66–1.76 (m, 5H), 1.55–1.63 (m, 3H), 1.24–1.26 (m, 3H), 1.10–1.12 (m, 1H), 0.85–0.92 (m, 6H).

HRMS calcd $C_{25}H_{34}N_5O_4$ ($M + H$) $^+$: 468.2611; found 468.2618.

2-(4-(2,6-dioxo-1,3-dipropyl-2,3,6,7-tetrahydro-1H-purin-8-yl)phenoxy)-N-(pyridin-4-ylmethyl)acetamide (9). Compound **9** was synthesized following the general procedure using 4-(methylamino)pyridine and obtaining 11.0 mg of pure compound (45% yield).

1H NMR ($DMSO$, 400 Hz) δ 8.79 (t, 1H, $J = 5.7$ Hz), 8.47 (d, 2H, $J = 5.6$ Hz), 8.08 (d, 2H, $J = 8.8$ Hz), 7.23 (d, 1H, $J = 5.5$ Hz), 7.12 (d, 2H, $J = 8.7$ Hz, 2H), 4.68 (s, 2H), 4.37 (d, 2H, $J = 6.1$ Hz), 4.02 (t, 2H, $J = 7.2$ Hz), 3.87 (t, 2H, $J = 7.0$ Hz), 1.74 (q, 2H, $J = 7.4$, 14.5 Hz), 1.58 (q, 2H, $J = 7.3$, 14.4 Hz), 0.85–0.92 (m, 6H).

HRMS calcd $C_{25}H_{29}N_6O_4$ ($M + H$) $^+$: 477.2250; found 477.2243.

2-(4-(2,6-dioxo-1,3-dipropyl-2,3,6,7-tetrahydro-1H-purin-8-yl)phenoxy)-N-(pyrazin-2-yl)acetamide (10). Compound **10** was synthesized following the general procedure using aminopyrazine and obtaining 6.5 mg of pure compound (27% yield).

1H NMR ($DMSO$, 400 Hz) δ 10.97 (s, 1H), 9.30 (s, 1H), 8.44 (s, 1H),

8.40 (s, 1H), 8.07 (d, 2H, $J = 8.7$ Hz), 7.11 (d, 2H, $J = 8.7$ Hz, 2H), 4.94 (s, 2H), 2.38 (t, 2H, $J = 7.1$ Hz), 3.86 (t, 2H, $J = 7.2$ Hz), 1.73 (q, 2H, $J = 7.4$, 14.5 Hz), 1.58 (q, 2H, $J = 7.3$, 14.4 Hz), 0.85–0.92 (m, 6H).

HRMS calcd $C_{23}H_{26}N_7O_4$ ($M + H$)⁺: 464.2046; found 464.2047.

2-(4-(2,6-dioxo-1,3-dipropyl-2,3,6,7-tetrahydro-1H-purin-8-yl)phenoxy)-N-(4-methylbenzyl)acetamide (20). Compound 20 was synthesized following the general procedure using 4-methylbenzylamine and obtaining 44.5 mg of pure compound (91% yield).

¹H NMR (DMSO, 300 Hz) δ 8.64 (t, 1H, $J = 5.9$ Hz), 8.07 (d, 2H, $J = 8.8$ Hz), 7.16–7.08 (m, 6H), 4.63 (s, 2H), 4.30 (d, 2H, $J = 5.9$ Hz), 4.02 (t, 2H, $J = 7.0$ Hz), 3.87 (t, 2H, $J = 7.3$ Hz), 2.26 (s, 3H), 1.74 (m, 2H), 1.58 (m, 2H), 0.91 (t, 3H, $J = 7.6$ Hz), 0.88 (t, 3H, $J = 7.7$ Hz).

HRMS calcd $C_{27}H_{32}N_5O_4$ ($M + H$)⁺: 490.2454; found 490.2462.

2-(4-(2,6-dioxo-1,3-dipropyl-2,3,6,7-tetrahydro-1H-purin-8-yl)phenoxy)-N-(4-fluorobenzyl)acetamide (21). Compound 21 was synthesized following the general procedure using 4-fluorobenzylamine and obtaining 32.3 mg of pure compound (65% yield).

¹H NMR (DMSO, 300 Hz) δ 8.71 (t, 1H, $J = 5.9$ Hz), 8.07 (d, 2H, $J = 8.8$ Hz), 7.30 (dd, 2H, $J = 5.9$, 8.5 Hz), 7.16–7.08 (m, 4H), 4.64 (s, 2H), 4.33 (d, 2H, $J = 6.0$ Hz), 4.02 (t, 2H, $J = 7.1$ Hz), 3.87 (t, 2H, $J = 7.3$ Hz), 1.74 (m, 2H), 1.58 (m, 2H), 0.91 (t, 3H, $J = 7.6$ Hz), 0.88 (t, 3H, $J = 7.6$ Hz).

HRMS calcd $C_{26}H_{29}FN_5O_4$ ($M + H$)⁺: 494.2204; found 494.2199.

N-(4-bromobenzyl)-2-(4-(2,6-dioxo-1,3-dipropyl-2,3,6,7-tetrahydro-1H-purin-8-yl)phenoxy)acetamide (22). Compound 22 was synthesized following the general procedure using 4-bromobenzylamine and obtaining 30.0 mg of pure compound (54% yield).

¹H NMR (DMSO, 300 Hz) δ 8.75 (t, 1H, $J = 6.1$ Hz), 8.09 (d, 2H, $J = 8.7$ Hz), 7.47–7.40 (m, 2H), 7.27 (d, 2H, $J = 4.9$ Hz), 7.10 (d, 2H, $J = 8.9$ Hz), 4.66 (s, 2H), 4.35 (d, 2H, $J = 6.1$ Hz), 4.02 (t, 2H, $J = 7.1$ Hz), 3.87 (t, 2H, $J = 7.3$ Hz), 1.74 (m, 2H), 1.58 (m, 2H), 0.91 (t, 3H, $J = 7.5$ Hz), 0.88 (t, 3H, $J = 7.6$ Hz).

HRMS calcd $C_{26}H_{29}BrN_5O_4$ ($M + H$)⁺: 554.1403; found 554.1397.

N-(3,4-dihydroxybenzyl)-2-(4-(2,6-dioxo-1,3-dipropyl-2,3,6,7-tetrahydro-1H-purin-8-yl)phenoxy)acetamide (23). Compound 23 was synthesized following the general procedure using 3,4-dihydroxybenzylamine hydrobromide and obtaining 18.7 mg of pure compound (37% yield).

¹H NMR (DMSO, 300 Hz) δ 8.53 (t, 1H, $J = 6.0$ Hz), 8.06 (d, 2H, $J = 8.9$ Hz), 7.08 (d, 2H, $J = 8.8$ Hz), 6.69 (d, 1H, $J = 1.8$ Hz), 6.65 (d, 1H, $J = 8.0$ Hz), 6.51 (dd, 1H, $J = 8.1$, 1.9 Hz), 4.59 (s, 2H), 4.17 (d, 2H, $J = 6.0$ Hz), 4.01 (t, 2H, $J = 7.2$ Hz), 3.86 (t, 2H, $J = 7.3$ Hz), 1.74 (m, 2H), 1.58 (m, 2H), 0.90 (t, 3H, $J = 7.4$ Hz), 0.87 (t, 3H, $J = 7.6$ Hz).

HRMS calcd $C_{26}H_{30}N_5O_6$ ($M + H$)⁺: 508.2196; found 508.2184.

(R)-2-(4-(2,6-dioxo-1,3-dipropyl-2,3,6,7-tetrahydro-1H-purin-8-yl)phenoxy)-N-(1-phenylethyl)acetamide (24). Compound 24 was synthesized following the general procedure using R-(+)- α -methylbenzylamine and obtaining 28.6 mg of pure compound (58% yield).

¹H NMR (DMSO, 300 Hz) δ 8.57 (d, 1H, $J = 8.4$ Hz), 8.06 (d, 2H, $J = 8.7$ Hz), 7.33–7.20 (m, 5H), 7.08 (d, 2H, $J = 8.7$ Hz), 5.01 (m, 1H), 4.61 (s, 2H), 4.02 (t, 2H, $J = 7.1$ Hz), 3.87 (t, 2H, $J = 7.3$ Hz), 1.74 (m, 2H), 1.58 (m, 2H), 1.41 (d, 3H, $J = 6.9$ Hz), 0.90 (t, 3H, $J = 7.6$ Hz), 0.88 (t, 3H, $J = 7.8$ Hz).

HRMS calcd $C_{27}H_{32}N_5O_4$ ($M + H$)⁺: 490.2454; found 490.2433.

(S)-2-(4-(2,6-dioxo-1,3-dipropyl-2,3,6,7-tetrahydro-1H-purin-8-yl)phenoxy)-N-(1-phenylethyl)acetamide (25). Compound 25 was synthesized following the general procedure using S-(-)- α -methylbenzylamine and obtaining 22.0 mg of pure compound (45% yield).

¹H NMR (DMSO, 300 Hz) δ 8.57 (d, 1H, $J = 8.1$ Hz), 8.06 (d, 2H, $J = 8.7$ Hz), 7.33–7.20 (m, 5H), 7.08 (d, 2H, $J = 8.7$ Hz), 5.01 (m, 1H), 4.61 (s, 2H), 4.02 (t, 2H, $J = 7.1$ Hz), 3.87 (t, 2H, $J = 7.2$ Hz), 1.74 (m, 2H), 1.58 (m, 2H), 1.41 (d, 3H, $J = 7.0$ Hz), 0.90 (t, 3H, $J = 7.6$ Hz), 0.88 (t, 3H, $J = 7.7$ Hz).

HRMS calcd $C_{27}H_{32}N_5O_4$ ($M + H$)⁺: 490.2454; found 490.2429.

General procedure for the preparation of compound 29. N-(4-Aminophenyl)-2-(4-(2,6-dioxo-1,3-dipropyl-2,3,6,7-tetrahydro-1H-purin-8-yl)phenoxy)acetamide (**28**) was prepared reacting XCC with p-phenylenediamine in the presence of EDAC and DMAP as carboxyl group activating agents. Due to the chemical sensitivity of this particular p-amino-anilide bond, after work-up of the reaction mixture, compound **28** was directly used in the successive step without further purification. Reaction of the latter with thiophosgene furnished compound **29** (2-(4-(2,6-dioxo-1,3-dipropyl-2,3,6,7-tetrahydro-1H-purin-8-yl)phenoxy)-N-(4-isothiocyanatophenyl)acetamide).

N-(4-Aminophenyl)-2-(4-(2,6-dioxo-1,3-dipropyl-2,3,6,7-tetrahydro-1H-purin-8-yl)phenoxy)acetamide (28). A solution of XCC (0.06 mmol, **1**), p-phenylenediamine (0.06 mmol), EDAC (0.130 mmol), and DMAP (0.130 mmol) in 1 mL of anhydrous DMF was stirred at room temperature for 18 h. The following day, a sample of the solution was withdrawn for MS-LC analysis showing complete conversion to compound **28**. Water (2 mL) was added to the solution with formation of a white solid that was filtered and washed three times with ether (26 mg, 90 %).

HRMS calcd $C_{25}H_{29}N_6O_4$ ($M + H$)⁺: 477.2316; found 477.2311.

2-(4-(2,6-dioxo-1,3-dipropyl-2,3,6,7-tetrahydro-1H-purin-8-yl)phenoxy)-N-(4-isothiocyanatophenyl)acetamide (29). To a suspension of **28** (0.05 mmol) in 8 mL of $CHCl_3$ and $NaHCO_3$ saturated water solution (3:1) was added thiophosgene (0.33 mmol) all at once under vigorous stirring, and the mixture stirred at room temperature for 5 min. Then, additional $CHCl_3$ (20 mL) and water (5 mL) were added to break the emulsion. The phases were separated, and the aqueous phase was washed with $CHCl_3$ (3 \times 25 mL). The organic phases were combined, dried over Na_2SO_4 and the solvent removed under vacuum to obtain 6.6 mg (25% yield) of the pure compound **29**.

¹H NMR ($CDCl_3$, 400 Hz) δ 10.5. (s, 1H), 8.20 (d, $J = 0.02$ Hz, 2H), 7.82 (d, $J = 0.02$ Hz, 2H), 7.51 (d, $J = 0.02$ Hz, 2H), 7.21 (d, $J = 0.02$ Hz, 2H), 4.90 (s, 2H), 4.13 (t, $J = 0.02$ Hz, 2H), 3.95 (t, $J = 0.02$ Hz, 2H), 1.85 (q, $J = 0.03$ Hz, 2H), 1.48 (q, $J = 0.03$ Hz, 2H), 0.90–1.09 (m, 4H).

2.2. Biology

2.2.1. Chemicals and reagents

Bovine serum albumin (BSA) and the bicinchoninic acid (BCA) protein assay kit were purchased from Fisher Scientific (Hampton, New Hampshire, United States). [³H]PSB-603 (specific activity 79 Ci $mmol^{-1}$) was custom-labeled and purchased from Quotient BioResearch (Waltham, MA) and ZM241385 was a kind gift by Zeneca Pharmaceuticals (Macclesfield, United Kingdom). Adenosine deaminase (ADA) was purchased from Sigma Aldrich (Zwijndrecht, the Netherlands). All other chemicals used in the biological experiments were purchased from standard commercial sources.

CHO-spap cells either “empty” or stably expressing the wildtype human $A_{2B}AR$ (CHO-spap- $hA_{2B}AR$) were kindly provided by S.J. Dowell, Glaxo Smith Kline.

2.2.2. Cell culture

CHO-spap cells were grown in Dulbecco’s modified Eagle’s medium: Nutrient Mixture F-12 (DMEM/F12) supplemented with 10% (v/v) newborn calf serum, 100 IU/mL penicillin and 100 μ g/mL streptomycin at 37 °C and 5% CO_2 . Cells were subcultured at a ratio of 1:20 twice weekly. CHO-spap- $hA_{2B}AR$ cells were grown in the same medium supplemented with 1 mg/mL G418 and 0.4 mg/mL hygromycin. Cells were subcultured at a ratio of 1:20 twice weekly.

2.2.3. Membrane preparation

CHO-spap- $hA_{2B}AR$ cells were cultured as a monolayer in 15 cm ϕ plates to about 90% confluency. Cells were removed from the plates by scraping into 5 mL of phosphate-buffered saline (PBS) and centrifuged for 5 min at 1500 rpm. The resulting pellets were resuspended in ice-cold Tris-HCl buffer (50 mM Tris-HCl, pH 7.4) and homogenized using an

Ultra Turrax homogenizer (IKA Werke GmbH & Co.KG, Staufen, Germany). Centrifugation at 31,000 rpm in an Optima LE-80 K ultracentrifuge with Ti-70 rotor (Beckman Coulter, Fullerton, CA) at 4 °C for 20 min, resulted in separation of membranes and cytosolic fraction. Subsequently, pellet was resuspended in 10 mL Tris-HCl buffer, homogenized and centrifuged once again. The final pellet was suspended in assay buffer (50 mM Tris-HCl buffer, 0.1% (w/v) CHAPS, pH 7.4), ADA was added to break down endogenous adenosine, and the homogenization step was repeated. Aliquots were stored at -80C and the membrane protein concentration was determined by a BCA protein determination assay [26]. The BCA results were measured in a Wallac EnVision 2104 Multilabel Reader (Perkin Elmer, Groningen, The Netherlands).

2.2.4. Radioligand binding assay

In all radioligand binding experiments, CHO-spap-hA_{2B}AR membranes were thawed and homogenized using an Ultra Turrax homogenizer at 24,000 rpm (IKA-Werke GmbH & Co.KG, Staufen, Germany), diluted in assay buffer to the desired concentration (10–30 µg per well or Eppendorf tube). All materials were brought to 25 °C, 30 min prior to the experiment. ZM241385 (10 µM) was used to determine nonspecific binding (NSB). DMSO concentrations were 2% for all compounds except for **8**, **12–18** and **20–22**, where the concentration was 0.25%. The two different DMSO concentrations had negligible effects on the radioligand binding results. Finally, total radioligand binding (TB) did not exceed 10% of the [³H]PSB-603 present in the assay in order to prevent ligand depletion.

2.2.4.1. Displacement experiments. Were performed using 1.5 nM [³H]PSB-603 and a competing unlabeled ligand at multiple concentrations diluted in assay buffer (50 mM Tris-HCl, 0.1% (w/v) CHAPS, pH 7.4). Binding was initiated by addition of CHO-spap-hA_{2B}AR membrane aliquots to reach a total volume of 100 µL. Samples were incubated at 25 °C for 2 h to reach equilibrium. The incubation was terminated by rapid vacuum filtration over 96-well Whatman GF/C filter plates using a PerkinElmer Filtermate harvester (PerkinElmer, Groningen, Netherlands). Filters were subsequently washed ten times using ice-cold wash buffer (50 mM Tris-HCl, 0.1% (w/v) BSA, pH 7.4). Filter plates were dried at 55 °C for about 45 min and afterwards 25 µL Microscint (PerkinElmer) was added per well. Filter-bound radioactivity was determined by liquid scintillation spectrometry using a 2450 Microbeta² scintillation counter (PerkinElmer).

2.2.4.2. Saturation binding experiments. Were carried out by incubating increasing concentrations of [³H]PSB-603 (from 0.05 to 5 nM) with membrane aliquots for 2 hr at 25 °C. Non-specific binding was assessed by three concentrations of the radioligand (0.05 nM, 1 nM and 5 nM) and analyzed by linear regression. Incubation was terminated by filtration through GF/C filters using a Brandel-harvester (Brandel Harvester 24w, Gaithersburg, MD, USA). Filters were washed three times using ice-cold wash buffer and collected in tubes. 3.5 mL Emulsifier-Safe scintillation fluid (Perkin Elmer, Groningen, the Netherlands) was added and the filter-bound radioactivity was determined in a Tri-Carb 2900TR liquid scintillation analyzer (PerkinElmer).

2.2.4.3. Association experiments. Were performed by incubation of [³H]PSB-603 (1.5 nM) with membrane aliquots at 25 °C. The amount of receptor-bound radioligand was determined after filtration at different time intervals for a total incubation time of 45 min and samples were obtained as described under “Displacement experiments”.

2.2.4.4. Dissociation experiments. Were carried out after a 45 min pre-incubation of 1.5 nM [³H]PSB-603 and membrane aliquots. Subsequently, dissociation of the radioligand at different time points up to 150 min was initiated by addition of 5 µL ZM241385 (assay

concentration 10 µM). Dissociation experiments were performed at 25 °C. The amount of receptor-bound radioligand was determined after filtration and samples were obtained as described under “Displacement experiments”.

2.2.4.5. Competition association experiments. Were performed at 25 °C and in a total volume of 100 µL, by incubation of 1.5 nM [³H]PSB-603 and a competing ligand diluted in assay buffer to reach IC₅₀ concentration. Addition of CHO-spap-hA_{2B}AR membrane aliquots initiated the association. The amount of receptor-bound radioligand was determined at different time points up to 3 hr. After 3 hr the incubation was terminated and samples were obtained as described under “Displacement experiments”.

2.2.4.6. Washout experiments. Were performed at 25 °C and in a total volume of 400 µL. CHO-spap-hA_{2B}AR membranes were incubated for 2 hr with the unlabeled compounds (at a final concentration of 10 × IC₅₀) while shaking at 1,000 RPM in an Eppendorf thermomixer comfort (Eppendorf AG, Hamburg, Germany). Subsequently, the samples were centrifuged at 13200 rpm (16 100g) at 4 °C for 5 min and the supernatant containing unbound ligand was removed. Pellets were resuspended in 1 mL of assay buffer, and samples were incubated for 10 min at 25 °C in the thermomixer. After four centrifugation and washing cycles in total, supernatant was discarded and the membranes were resuspended in a total volume of 400 µL containing 1.5 nM [³H]PSB-603. After 2 hr at 25 °C incubations were terminated by rapid filtration through GF/C filters using a Brandel harvester and the samples were obtained as described under “Saturation binding experiments”.

2.2.5. Label-free whole-cell assay

2.2.5.1. Detection principle. Label-free assays were performed using the xCELLigence real-time cell analyser (RTCA) system [27,28], as described previously [29]. In short, cells attached to the gold-coated electrodes embedded on the bottom of E-plates are generating electrical impedance which is monitored by the RTCA system. Variations in cell number, adhesion, viability and morphology result in impedance changes (Z) which are constantly recorded at 10 kHz. Z is displayed in the unitless parameter called Cell Index (CI) [28,30], which is defined as $(Z_i - Z_0) / 15 \Omega$. Z_i is the impedance at a given time point and Z_0 represents the baseline impedance in the absence of cells, which is measured prior to the start of the experiment.

2.2.5.2. Determination of pEC₅₀ value of NECA for hA_{2B}AR. CHO-spap and CHO-spap-hA_{2B}AR cells were harvested and centrifuged at 200x g (1500 rpm) for 5 min. Z_0 was measured in the presence of 45 µL culture media in 96 well PET E-plates (Bioké, Leiden, The Netherlands). 60,000 cells were seeded in a volume of 50 µL per well. After maintaining at room temperature for about 30 min, the E-plate was placed into the recording station housed in a 37 °C and 5% CO₂ incubator. Impedance was measured every 15 min. After about 19 hr 30 min of recording, cells were treated with NECA (10⁻¹¹ till 10⁻⁶ M) or vehicle control (0.25% DMSO) in 5 µL. CI was recorded for 90 min (recording schedule: 15 s intervals for 25 min, followed by 1 min intervals for 20 min and 5 min intervals for 45 min).

2.2.5.3. Validation that NECA signaling is hA_{2B}AR-mediated. Z_0 was measured in the presence of 45 µL culture media in 96 well PET E-plates (Bioké, Leiden, The Netherlands). 60,000 CHO-spap or CHO-spap-hA_{2B}AR cells were seeded in a volume of 50 µL per well. The E-plate was left for about 30 min at room, and afterwards was placed into the recording station housed in a 37 °C and 5% CO₂ incubator. Impedance measurements were recorded every 15 min. After about 19 hr 30 min of recording, cells were pre-treated with saturating concentrations of an AR antagonist, i.e. A₁: DPCPX (45 nM); A_{2A}: SCH442416 (4.8 nM); A_{2B}:

PSB603 (55 nM); A3: PSB11 (230 nM) or vehicle control (vehicle 1; 0.25% DMSO) in 5 μ L. CI was recorded for 4 hr (recording schedule: 15 s intervals for 10 min, followed by 1 min intervals for 50 min and 15 min interval for 180 min). Subsequently, cells were treated with NECA (EC_{80}) or vehicle control (vehicle 2; 0.25% DMSO) in 5 μ L and CI was recorded for 90 min (recording schedule: 15 s intervals for 25 min, followed by 1 min intervals for 15 min and 5 min intervals for 50 min).

2.2.5.4. Determination of pIC_{50} values of $hA_{2B}AR$ antagonists. Z_0 was measured in the presence of 40 μ L culture media in 96 well PET E-plates (Bioké, Leiden, The Netherlands). CHO-spap- $hA_{2B}AR$ cells were seeded in a density of 60,000 cells per well (50 μ L). After staying 30 min without agitation at room temperature, the E-plate was placed into the recording station housed in a 37 °C and 5% CO_2 incubator. Impedance was measured every 15 min. After about 19 hr 30 min of recording, cells were pre-treated with $A_{2B}AR$ antagonists (10^{-9} till 10^{-5} M) or vehicle control (vehicle 1; 0.25% DMSO) in 5 μ L. CI was recorded for 4 hr (recording schedule: 15 s intervals for 10 min, followed by 1 min intervals for 50 min and 15 min interval for 180 min). Subsequently, cells were treated with NECA (EC_{80}) or vehicle control (vehicle 2; 0.25% DMSO) in 5 μ L and CI was recorded for 90 min (recording schedule: 15 s intervals for 25 min, followed by 1 min intervals for 15 min and 5 min intervals for 50 min).

2.2.5.5. Washout assay. The assay followed the same initial steps as described in “Determination of pIC_{50} values for $hA_{2B}AR$ antagonists”. After about 19 hr 30 min of recording, cells were pre-treated with $A_{2B}AR$ antagonists ($30 \times IC_{50}$; based on the pIC_{50} value determined with “Determination of pIC_{50} values for $hA_{2B}AR$ antagonists”) or vehicle control (vehicle 1; 0.25% DMSO) in 5 μ L. CI was recorded for 4 hr (recording schedule: 15 s intervals for 10 min, followed by 1 min intervals for 50 min and 15 min intervals for 180 min). Subsequently, wells were washed by aspiration of the medium, followed by the addition of 95 μ L fresh serum free medium. For the unwashed cells, the medium was not removed but was pipetted up and down to simulate any mechanical cell stress. The E-plate was placed on the recording station and CI was recorded for 30 min (recording schedule: 15 s intervals for 25 min, followed by 1 min intervals for 5 min). Finally, cells were treated with NECA (EC_{80}) or vehicle control (vehicle 2; 0.25% DMSO) in 5 μ L and CI was recorded for 90 min (recording schedule: 15 s intervals for 25 min, followed by 1 min intervals for 15 min and 5 min intervals for 50 min).

2.3. Data analysis

2.3.1. Radioligand binding assays

Data analyses were performed using GraphPad Prism 8.0 software (GraphPad Software Inc., San Diego, CA, USA). For saturation assays, K_D and B_{max} values were determined by non-linear regression curve fitting using the one site: “total and non-specific binding” equation. For displacement assays, pIC_{50} values were obtained by non-linear regression curve fitting to a sigmoidal concentration–response curve using the “log(inhibitor) vs. response” GraphPad analysis equation. pK_i values were converted from pIC_{50} values and the saturation K_D using the Cheng–Prusoff equation [31]:

$$K_i = IC_{50} / (1 + [\text{radioligand}] / K_D)$$

The k_{off} value was obtained using a one-phase exponential decay analysis of data resulting from a radioligand dissociation assay. The value of k_{on} was determined using the equation:

$$k_{on} = (k_{obs} - k_{off}) / [\text{radioligand}]$$

in which k_{obs} was determined using a one phase association analysis of data from a radioligand association assay. The association and dissociation rate constants were used to calculate the kinetic K_D value using: $K_D = k_{off} / k_{on}$.

Association and dissociation rate constants for unlabelled $A_{2B}AR$ inhibitors were determined by nonlinear regression analysis of competition association data as described by Motulsky and Mahan [32]. The data were fitted into the GraphPad “kinetics of competitive binding” analysis, where k_1 and k_2 are the k_{on} ($M^{-1}min^{-1}$) and k_{off} (min^{-1}) of [3H]PSB-603 obtained from radioligand association and dissociation assays, respectively, L is the radioligand concentration (nM), I is the concentration of unlabeled competitor (nM), X is the time (min) and Y is the specific binding of the radioligand (DPM). Fixing these parameters resulted in the calculation of the following parameters: k_3 , which is the k_{on} value ($M^{-1}min^{-1}$) of the unlabeled ligand; k_4 , which is the k_{off} value (min^{-1}) of the unlabeled ligand and B_{max} , that equals the total binding (DPM). All competition association data were globally fitted. The residence time (RT) was calculated using $RT = 1 / k_{off}$ [33].

All values are shown as mean \pm S.E.M. of at least three independent experiments performed in duplicate. Statistical analysis was performed if indicated, using a one-way ANOVA with Dunnett’s post-test (**** $P < 0.0001$; *** $P < 0.001$; ** $P < 0.01$; * $P < 0.05$) or an unpaired Student’s *t* test (#### $P < 0.0001$; ### $P < 0.001$; ## $P < 0.01$; # $P < 0.05$). Observed differences were considered statistically significant if P-values were below 0.05.

2.3.2. Label-free whole-cell assay

RTCA software 2.0 (ACEA Biosciences, Inc.) was used to record all experimental data. Data were analyzed using GraphPad Prism 8.0. Compound responses, baseline-corrected to vehicle control, were normalized at the time of ligand addition to obtain Normalized Cell Index (NCI) values to correct for compound-independent responses. The time of normalization was either at approximately 19 hr 30 min, at 23 hr 30 min or at 24 hr after cell seeding for analysis of NECA response depending on the type of assay (number of steps), i.e. pre-treatment with antagonists, washing and NECA treatment, respectively.

The absolute values of Area Under the Curve (AUC) up to 90 min after NECA addition were exported from the RTCA software to GraphPad Prism 8.0 for further analysis yielding concentration–response curves. The pEC_{50} value of NECA (Table 5) was obtained using non-linear regression curve fitting of AUC data into “log(agonist) vs. response (three parameters)” analysis. pIC_{50} values of $hA_{2B}AR$ antagonists (Table 5) were obtained using non-linear regression curve fitting of AUC data into “log(inhibitor) vs. response (three parameters)” analysis. Data shown are the mean \pm S.E.M of at least three individual experiments performed in duplicate.

3. Results

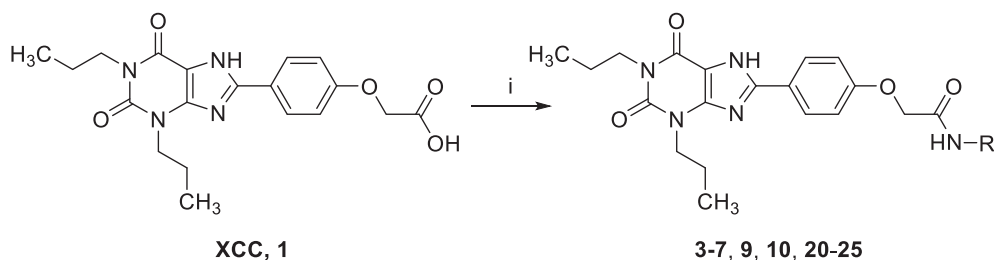
3.1. Chemistry

2-(4-(2,6-Dioxo-1,3-dipropyl-2,3,6,7-tetrahydro-1H-purin-8-yl)phenoxy)acetic acid (xanthine carboxylic congener, XCC, **1**) was synthesized as reported [24]. Its amide derivatives **3–7**, **9**, **10**, **20–25** were prepared by reaction with the desired amine in the presence of EDAC and DMAP as carboxyl group activating agents (Scheme 1). XCC was also used as the starting reagent for the synthesis of isothiocyanate-containing **29**, aimed to bind to the $A_{2B}AR$ covalently (Scheme 2).

3.2. Biological Evaluation

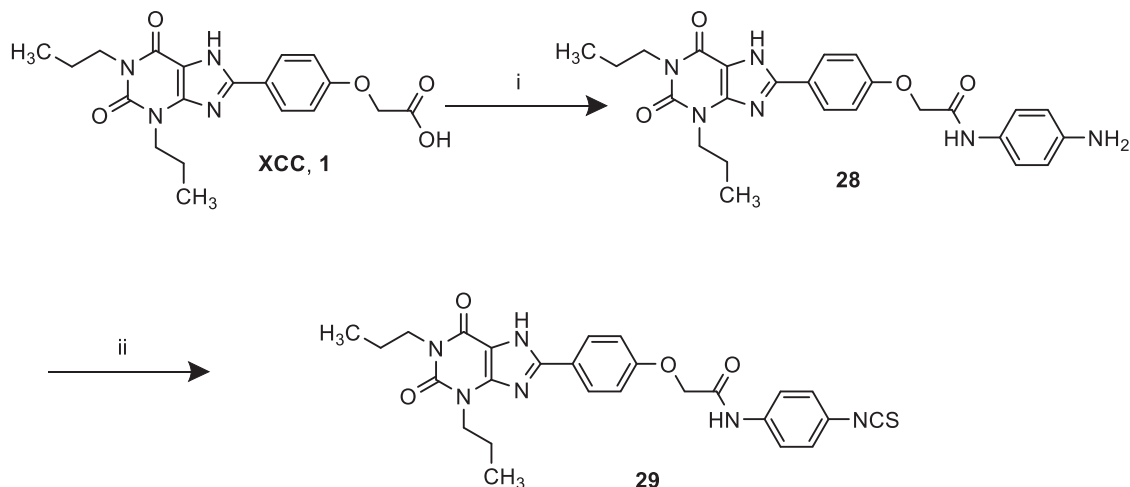
3.2.1. Validation of [3H]PSB-603 equilibrium and kinetic radioligand binding assays

Firstly, the binding profile of tritium-labeled $A_{2B}AR$ antagonist 8-[4-(4-(4-chlorophenyl)piperazine-1-sulfonyl) phenyl]-1-propylxanthine ([3H]PSB-603) was characterized on CHO-spap- $hA_{2B}AR$ membranes. In a saturation binding assay receptor binding was saturable and quantified by a K_D value of 1.71 nM and a B_{max} value of 4.30 pmol/mg (Fig. 1A, Table 1). When evaluated in a homologous displacement assay, unlabeled PSB-603 showed similar affinity, yielding a pK_i value of 8.90



Reagents and conditions: i. EDAC, DMAP, primary or secondary amine, DMF, rt, 18h

Scheme 1. Synthesis of XCC amides.



Reagents and conditions: i. EDAC, DMAP, p-phenylene diamine, DMF, rt, 18 h; ii. thiophosgene, NaHCO₃ sat. aq. sol., CHCl₃, rt, 5 min.

Scheme 2. Synthesis of compound **29**, designed as covalently binding antagonist.

(Fig. 1D, Table 1).

Subsequently, [³H]PSB-603 was evaluated in kinetic binding assays in order to determine its kinetic binding parameters k_{on} and k_{off} (Fig. 1B, Table 1). [³H]PSB-603 associated rapidly to the hA_{2B}AR and equilibrium binding was reached within 20 min, while complete dissociation was reached within 55 min, resulting in a k_{off} value of 0.075 min⁻¹. The association and dissociation experiments resulted in the calculation of k_{on} and RT values of 0.096 nM⁻¹ min⁻¹ and 13 min, respectively. Based on the kinetic data a dissociation constant (kinetic K_D) was calculated to be 0.78 nM.

To obtain kinetic binding parameters for unlabeled A_{2B}AR antagonists, a radioligand competition association assay was developed. The specific binding of [³H]PSB-603 was measured in the absence and presence of unlabeled PSB-603 over a time course of 45 min (Fig. 1C) and k_{on} , k_{off} and kinetic K_D values of unlabeled PSB-603 were calculated to be 0.109 nM⁻¹ min⁻¹, 0.084 min⁻¹ and 0.77 nM, respectively (Table 1). As the values of the competition association assay were in excellent agreement with the ones from the association and dissociation assay (Table 1), the first was deemed validated for determining an unlabeled ligand's binding kinetics.

In order to increase the throughput of the assay, a single concentration of PSB-603 (1.0-fold its IC₅₀) was tested. Association and dissociation rate constants were found to be similar to the aforementioned ones, i.e. 0.111 ± 0.014 nM⁻¹ min⁻¹ and 0.086 ± 0.007 min⁻¹ for k_{on} and k_{off} respectively (data not shown). Consequently, all other compounds were tested only at one concentration equal to 1.0-fold their IC₅₀ determined from displacement experiments.

3.2.2. Determination of equilibrium binding affinity (K_i values) of A_{2B}AR antagonists

Once the necessary assays were developed and validated, various xanthine-based A_{2B}AR antagonists were examined. The affinities of all compounds were evaluated in an equilibrium radioligand displacement study using [³H]PSB-603 as the radiolabeled competitor. All compounds fully displaced the radioligand from the hA_{2B} receptor in a concentration-dependent manner. The data were fitted in a one-phase competition model showing mono-phasic displacement. A wide spread of affinities was noticed, ranging from 61.4 μM for compound **4** to 1.78 nM for compound **13**; all affinities are listed in Tables 2-4.

3.2.3. Evaluation of kinetic binding parameters (k_{on} , k_{off} , RT) of A_{2B}AR antagonists

Any compound with a K_i value < 100 nM was assessed in kinetic binding assays, i.e. competition association assay. The k_{on} values of the 15 qualifying compounds exhibited a 26-fold range, spanning from 0.0014 nM⁻¹ min⁻¹ for **14** to 0.036 nM⁻¹ min⁻¹ for **3**. On the contrary, k_{off} values displayed a greater 94-fold variation, with compounds **17** and **3** defining the lower and upper limits, i.e. 0.011 min⁻¹ and 1.071 min⁻¹, respectively.

3.2.4. Evaluation of ligand binding recovery with a washout assay

To validate the results of the competition association assay and distinguish between ligands with distinct kinetic binding parameters, a [³H]PSB-603 washout assay was developed (Fig. 2, Table 5). Compounds **18** and **17** were selected as they presented a short (8 min) and

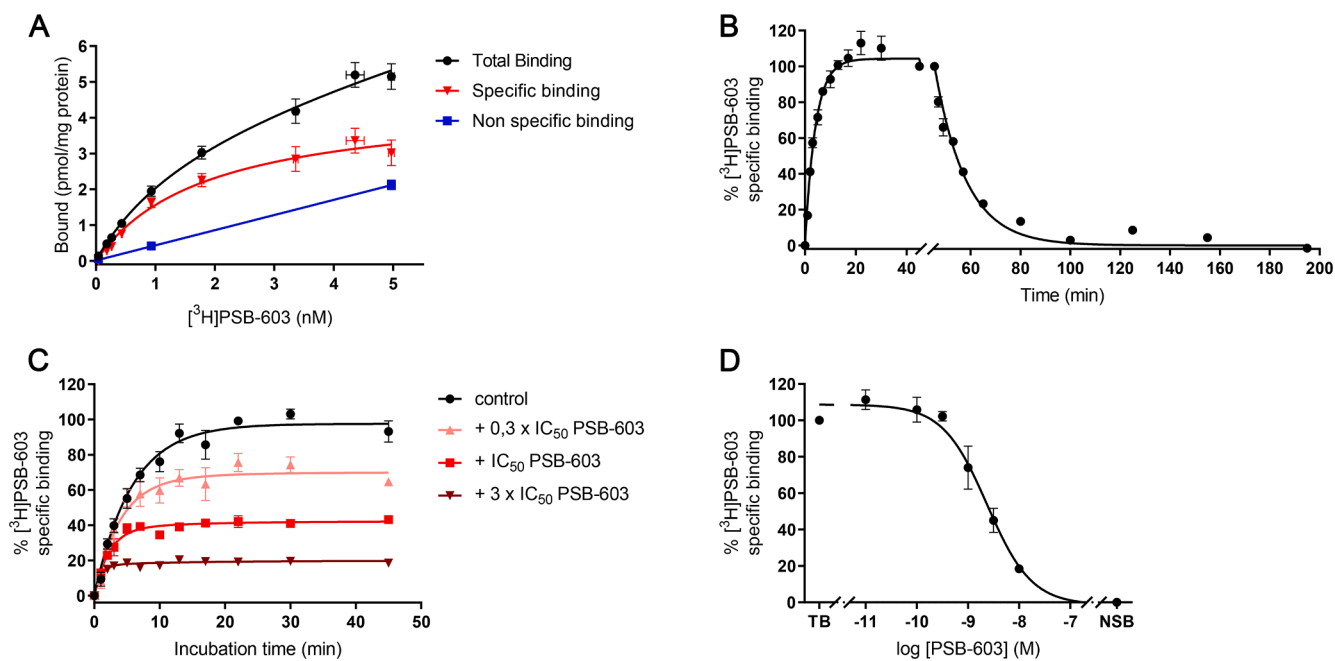


Fig. 1. Characterization of [³H]PSB-603 binding to hA_{2B}AR expressed on CHO-spap-hA_{2B}AR membranes at 25 °C. (A) Binding of [³H]PSB-603 in an equilibrium saturation assay. (B) Association and dissociation kinetics of 1.5 nM [³H]PSB-603 to and from hA_{2B}AR (100% equals to approx. 1700 dpm). (C) Competition association assay of [³H]PSB-603 in the absence or presence of 0.3x, 1x, and 3x IC₅₀ of unlabeled PSB-603 (100% equals to approx. 1700 dpm). (D) Homologous displacement of [³H]PSB-603 from hA_{2B}AR (100% equals to approx. 1900 dpm). Data are shown as mean ± S.E.M. from at least three independent experiments performed in duplicate.

Table 1

Comparison of the affinity, dissociation constants and kinetic parameters of PSB-603, obtained with different radioligand binding assays performed on CHO-spap-hA_{2B}AR membranes.

Assay	B _{max} (pmol/ mg)	K _D (nM)	pK _i (K _i (nM))	k _{on} (nM ⁻¹ min ⁻¹)	k _{off} (min ⁻¹)	RT (min)
Saturation binding	4.30 ± 0.30	1.71 ± 0.14	–	–	–	–
Displacement	–	–	8.90 ± 0.10 (1.25)	–	–	–
Association and dissociation	–	0.78 ± 0.09 ^a	–	0.096 ± 0.010	0.075 ± 0.003	13 ± 0.6
Competition association	–	0.77 ± 0.10 ^a	–	0.109 ± 0.008 ^b	0.084 ± 0.009 ^b	12 ± 1.3

Values are mean ± S.E.M. of at least three individual experiments performed in duplicate. ^aKinetic affinity values (K_D) determined by association and dissociation, and competition association assay, is defined as K_D = k_{off}/k_{on}. ^bKinetic parameters of unlabeled PSB-603 were determined by addition of 0.3-, 1- and 3-fold its IC₅₀ value.

long (87 min) RT compound, respectively, while they have similar structures and affinities. Compound **29**, designed as a putative covalently binding antagonist was also tested in this assay.

Both the washed and the unwashed conditions were assessed. For the washed condition, the unlabeled compounds were incubated with the target for 2 hr, followed by four wash and centrifugation cycles. Subsequently, [³H]PSB-603 was co-incubated which led to competition of the radioligand with the unlabeled ligand still bound after the washing procedure. For the unwashed condition no washing was performed before the determination of radioligand displacement. Based on the experimental set-up, the long RT compound and the covalent ligand would be predicted to remain bound to A_{2B}ARs, as they would not be

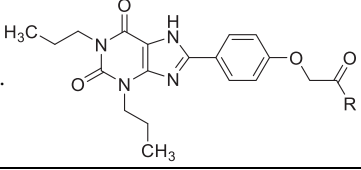
easily removed during the washing steps, and thus to result in lower radioligand binding.

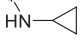
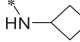
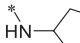
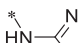
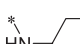
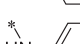


In the unwashed condition, all A_{2B}ARs were almost fully occupied by each of the compounds as there was little specific binding of [³H]PSB-603 observed (Fig. 2; control/unwashed). When the washed and unwashed conditions for both compounds **17** and **18** (Fig. 2; washed and unwashed) were compared, a significant increase in radioligand binding after washing was monitored, indicating that they had (partially) dissociated from the target and been washed away. This was hardly the case for compound **29**. The short RT compound **18** did not show any significant difference in specific [³H]PSB-603 binding compared to control (TB). Apparently, **18** was almost completely (85%) removed during the washing procedure. On the other hand, the long RT compound **17** was washed away for 56%, indicating that 44% of A_{2B}ARs were still occupied by this ligand after the applied washing cycles, showing a significant (*P* < 0.0001, Fig. 2, washed) decrease of [³H]PSB-603 specific binding compared to control (TB). This was even more apparent with compound **29**, with only 18% of material being washed off the receptor.

3.2.5. Structure-Affinity Relationships (SAR) and Structure-Kinetic Relationships (SKR)

We started with the study of the prototypic A_{2B}AR antagonist MRS1754 (**13**). In the displacement assay an affinity of 1.78 nM was determined. The kinetic characterization of **13** resulted in a determined RT of 69 min, which made us increase the duration of the competition association assay from 45 min to 3 h for all compounds in order to allow for the longer RT compounds to reach equilibrium.

We initiated the investigation on the xanthine scaffold with compound **1** [24]. Its affinity was found to be higher than 100 nM, the limit set as a threshold for the kinetic studies. By substitution of the acid moiety for an acetamide (**2**) the affinity increased approx. 7-fold. Therefore, this acetamide was incorporated in all other compounds synthesized and tested. For compound **2**, it was not possible to determine its kinetic characteristics, most probably because they were outside the detection range of our method.

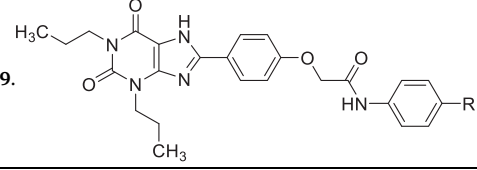
Table 2Affinity (pKi) and Kinetic Parameters (k_{on} , k_{off} , RT) of hA_{2B}AR antagonists **1** –


compd	R	pKi (Ki (nM))	k_{on} (nM ⁻¹ min ⁻¹)	k_{off} (min ⁻¹)	RT ^a (min)
1	OH	6.78 ± 0.06 (167)	n.d. ^b	n.d.	n.d.
2	NH ₂	7.60 ± 0.07 (25.1)	Kinetics outside the range of the assay (see text)		
3	* HN- 	7.44 ± 0.09 (36.3)	0.036 ± 0.006	1.071 ± 0.027	0.9 ± 0.0
4	* HN- 	4.21 ± 0.14 (61423)	n.d.	n.d.	n.d.
5	* HN- 	4.78 ± 0.17 (16749)	n.d.	n.d.	n.d.
6	* HN- 	5.26 ± 0.05 (5483)	n.d.	n.d.	n.d.
7	* HN- 	6.02 ± 0.09 (951)	n.d.	n.d.	n.d.
8	* HN- 	8.71 ± 0.01 (1.93)	0.015 ± 0.000	0.022 ± 0.006	46 ± 13
9	* HN- 	5.87 ± 0.16 (1351)	n.d.	n.d.	n.d.
10	* HN- 	5.16 ± 0.08 (6950)	n.d.	n.d.	n.d.
11	N (CH ₃ COOEt) ₂	6.95 ± 0.00 (113)	n.d.	n.d.	n.d.

Values represent the mean ± S.E.M. of at least three individual experiments, performed in duplicate. ^aRT = 1/ k_{off} . ^bn.d. = not defined.

Further functionalization of the acetamide to incorporate a cyclopropyl group (**3**) decreased the affinity, an effect observed for every non-aromatic ring tested (**3**, **4**, **5**, **7**). When pyrazole was incorporated (**6**) the affinity increased compared to compound **5**, but it remained in the micromolar range. To the contrary, introduction of pyridine (**9**) and pyrazine (**10**) decreased affinity even further when compared to the cyclohexyl substitution (**7**). Only incorporation of a phenyl ring (**8**) resulted in a low nanomolar affinity (1.93 nM) and a RT of 46 min. In addition to the cyclic substituents, a linear one (**11**) was incorporated, leading to a decrease in affinity compared to compound **2**. However, the affinity did not exceed the 100 nM threshold.

Taking these results into consideration we continued with *para* substitution of the phenyl ring and determined the influence of those substituents on affinity and kinetic binding parameters. When we substituted compound **8** with a *p*-methyl group (**12**) a slight decrease in affinity and a 10 min increase in RT were observed. Introduction of a *p*-cyano group (**13**) increased RT further, while the association rate constant increased about 4 times, yielding a compound with (sub)nanomolar affinity. The introduction of other electron withdrawing groups at the *p*-position (**14**, **15**, **16**, **17**, **18**) also yielded high affinity values for the receptor. Introduction of a nitro (**14**) or methyl ketone (**16**) substituent resulted in a moderate RT of 58 and 54 min, respectively, while the k_{on} value was largely varying, with **14** presenting a slow association to the receptor. The trifluoromethyl substituent (**15**) resulted in a high

Table 3Affinity (pKi) and Kinetic Parameters (k_{on} , k_{off} , RT) of hA_{2B}AR antagonists **12** –


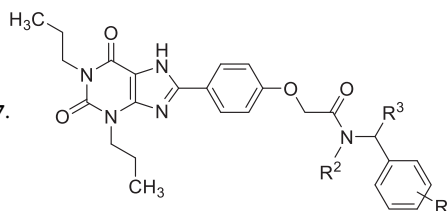
compd	R ¹	pKi (Ki (nM))	k_{on} (nM ⁻¹ min ⁻¹)	k_{off} (min ⁻¹)	RT ^a (min)	K_D ^b (nM)
12	CH ₃	8.47 ± 0.06 (3.42)	0.007 ± 0.002	0.018 ± 0.008	55 ± 25	2.7 ± 1.5
13	CN	8.75 ± 0.20 (1.78)	0.024 ± 0.005	0.015 ± 0.001	69 ± 2.4	0.61 ± 0.14
14	NO ₂	7.87 ± 0.04 (13.5)	0.0014 ± 0.0003	0.017 ± 0.006	58 ± 19	12 ± 4.9
15	CF ₃	8.54 ± 0.06 (2.86)	Kinetics outside the range of the assay (see text)			
16	COCH ₃	8.52 ± 0.05 (3.03)	0.011 ± 0.001	0.019 ± 0.006	54 ± 18	1.7 ± 0.58
17	COOCH ₃	8.64 ± 0.05 (2.29)	0.006 ± 0.001	0.011 ± 0.004	87 ± 29	1.8 ± 0.62
18	CONHCH ₃	7.70 ± 0.06 (19.9)	0.012 ± 0.001	0.125 ± 0.003	8.0 ± 0.2	10 ± 0.89
29	NCS	8.03 ± 0.05 (9.28)	Covalent mechanism (see text)			

Values represent the mean ± S.E.M. of at least three individual experiments, performed in duplicate. ^aRT = 1/ k_{off} . ^bKinetic K_D values, defined as $K_D = k_{off}/k_{on}$.

affinity for the receptor, while its kinetic characteristics could not be monitored due to the detection range of the assay. Introduction of a carboxylic acid (**17**) was responsible for the longest RT measured in this study, while a methylcarboxamide (**18**) resulted in a similar affinity but significantly shorter RT.

Subsequently, the introduction of a spacer between the acetamide and the phenyl ring was investigated (Table 4). By introducing a carbon linker (**19**) to compound **8**, the affinity dropped to a value in the micromolar range. A similar trend was observed for compounds **12** and **20**. Although affinity was decreased by 3-fold, it still remained in the nanomolar range for both compounds (**12** and **20**) allowing their kinetic characterization. The k_{on} value slightly decreased (0.007 nM⁻¹ min⁻¹ and 0.004 nM⁻¹ min⁻¹ for **12** and **20**, respectively), while RT was lessened by about 3-fold for **20**. Substitution of 4-methyl (**20**) by 4-fluoro (**21**), 4-bromo (**22**) and 3,4-di-hydroxy (**23**) did not lead to significant alteration of affinity, while RT remained to be 20 min or less. Only **21** yielded an increased k_{on} value, hence a faster association to hA_{2B}AR. Furthermore, the linker was altered by a methyl substitution on the R² position. The two enantiomers, R (**24**) and S (**25**), exhibited similar affinities and kinetic characteristics, with **24** showing approx. 2-fold increased k_{on} and k_{off} values compared to **25**, although the RT was short in both cases. When a phenyl ring was introduced on the R² position (**26**), the affinity slightly dropped compared to **24** and **25**, which after kinetic analysis appeared due to a decrease in association rate constant. The benzyl substitution of the amido group (**27**) resulted in an increase in affinity compared to the unsubstituted **19**, indicating that this benzyl moiety is well accommodated in the binding pocket of A_{2B}AR. However, when compared to **26**, **27** showed a lower affinity, suggesting that **27** did not optimally fit. Finally, **29**, bearing a reactive warhead, did not allow the determination of true equilibrium affinity

Table 4

Affinity (pK_i) and Kinetic Parameters (k_{on} , k_{off} , RT) of hA_{2B}AR antagonists **19** – **27**.

Cmpd	R ²	R ³	R ⁴	pK _i (K _i (nM))	k _{on} (nM ⁻¹ min ⁻¹)	k _{off} (min ⁻¹)	RT ^a (min)	K _D ^b (nM)
19	H	H	H	6.15 ± 0.15 (71.1)	n.d. ^c	n.d.	n.d.	n.d.
20	H	H	4-CH ₃	8.04 ± 0.04 (9.08)	0.004 ± 0.0015	0.046 ± 0.007	22 ± 3.5	12 ± 4.7
21	H	H	4-F	8.44 ± 0.06 (3.60)	0.017 ± 0.007	0.066 ± 0.015	15 ± 3.5	3.8 ± 1.7
22	H	H	4-Br	8.24 ± 0.11 (5.73)	0.007 ± 0.002	0.043 ± 0.019	23 ± 11	6.5 ± 3.6
23	H	H	3,4-diOH	7.61 ± 0.04 (24.4)	0.004 ± 0.001	0.099 ± 0.011	10 ± 1.1	27 ± 7.9
24^d	H	CH ₃	H	7.82 ± 0.07 (15.2)	0.022 ± 0.008	0.164 ± 0.042	6.1 ± 1.6	7.5 ± 3.9
25^d	H	CH ₃	H	8.09 ± 0.04 (8.11)	0.011 ± 0.003	0.097 ± 0.021	10 ± 2.3	8.6 ± 3.0
26	H		H	7.42 ± 0.18 (37.9)	0.0017 ± 0.0006	0.053 ± 0.017	19 ± 6.2	31 ± 16
27		H	H	6.92 ± 0.05 (11.9)	n.d.	n.d.	n.d.	n.d.

Values represent the mean ± S.E.M. of at least three individual experiments, performed in duplicate. ^aRT = 1/k_{off}. ^bKinetic K_D values, defined as K_D = k_{off}/k_{on}. ^cn.d. = not defined. ^dR- (**24**) or S- (**25**) enantiomer.

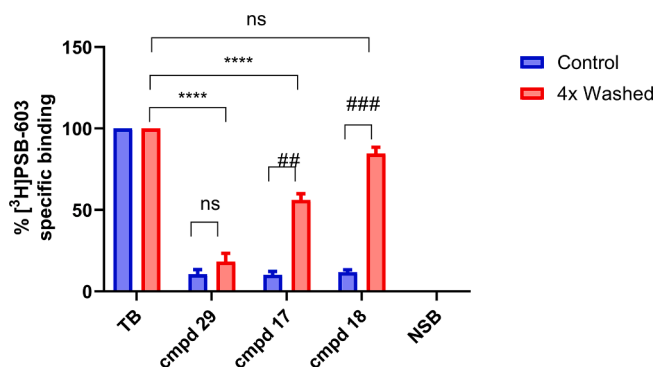


Fig. 2. Washout assays of compounds **17**, **18** and **29** at 25 °C. Recovery of radioligand binding in the presence of 10xIC₅₀ concentration of **17**, **18** or **29** after no (unwashed) and 4x (washed) washing. Data are shown as mean ± S.E.M. from at least three independent experiments performed in duplicate. The TB and NSB were normalized to 100% (approx. 8000 dpm) and 0% (approx. 2000 dpm) for each condition (control and 4x washed). One-way ANOVA was used for the multiple comparisons of 4x washed compounds to TB. ****p < 0.0001 t-test with Welch post-test was used for comparison between control and 4x washed condition for each compound. ##p < 0.01 ###p < 0.001.

values; its apparent affinity under the conditions tested was approx. 9 nM.

3.2.6. Correlation plots

To obtain a better comparison of kinetic and affinity parameters and understand their relationship, correlation plots for all compounds with measurable rate constants were constructed (Fig. 3). The affinity obtained from traditional radioligand displacement assay (pK_i) and the kinetic affinity (pK_D) derived from the radioligand competition association assay were found to be significantly and strongly correlated ($r = 0.95$, $P < 0.0001$; Fig. 3A), validating the use of the competition

Table 5

Potency values (pEC_{50} and pIC_{50}) of compounds in a label-free assay, and NECA signaling therein before and after washing, all on CHO-spap-hA_{2B}AR cells.

Compound	Label-free assay			
	pEC ₅₀ (EC ₅₀ (nM))	pIC ₅₀ (IC ₅₀ (nM))	washout - %AUC	
			unwashed	1x washed
NECA	8.95 ± 0.13 (1.12)	n.a.	100	100
17	n.a.	7.12 ± 0.13 (75.4)	10 ± 3	19 ± 6
18	n.a.	6.44 ± 0.21 (36.3)	12 ± 1	68 ± 7

Values represent the mean ± S.E.M. of at least three individual experiments, performed in duplicate. n.a. = not applicable.

association assay. When the association rate constants ($\log k_{on}$) of all kinetically characterized compounds were plotted against the kinetic affinity (Fig. 3B), a low, non-significant correlation was observed ($r = 0.36$, $P = 0.202$). However, the kinetic affinity was found to be significantly correlated with the dissociation rate constants (pK_{off}) ($r = 0.76$, $P = 0.0015$) (Fig. 3C).

3.2.7. Functional characterization of compounds **17** and **18**

Next to binding parameters we studied compounds **17** and **18** in a functional set-up, in order to investigate the link between binding kinetics and a possibly prolonged functional effect. For this purpose a label-free assay was developed as described in Materials and Methods and below.

Initial experiments with NECA (5'-N-ethylcarboxamidoadenosine), a non-selective AR agonist, were performed on control CHO-spap and CHO-spap-hA_{2B}ARs cells (Fig. 4). No response was found on "empty" CHO-spap cells upon treatment with NECA, whereas a concentration-dependent response was measured on CHO-spap-hA_{2B}ARs cells, yielding a pEC_{50} value of 8.95 (Table 5). In order to validate that the

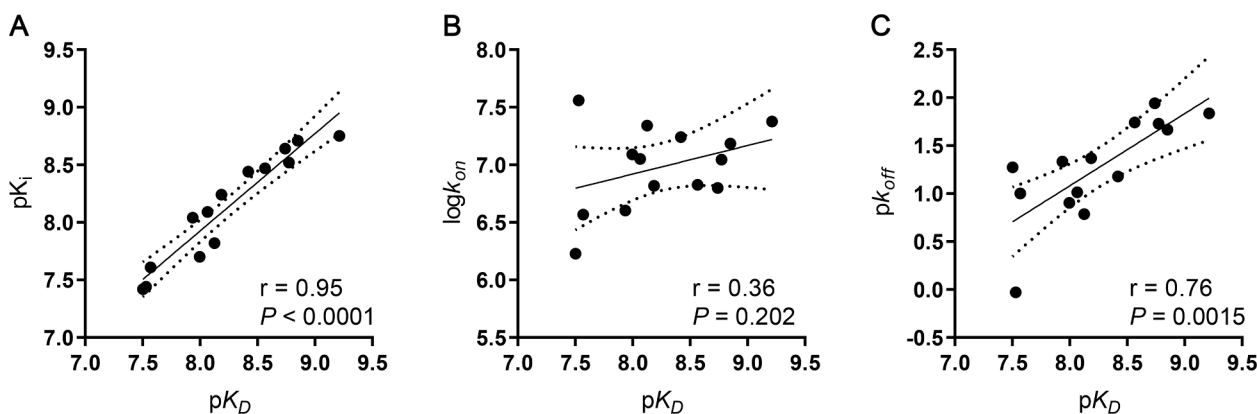


Fig. 3. Correlation plots between affinity and kinetic parameters. Kinetic affinity (pK_D) is plotted against (A) affinity determined from typical displacement assays (pK_i); (B) association rate constant ($\log k_{on}$); (C) dissociation rate constant (pK_{off}). The solid line corresponds to the linear regression of the data and the dotted lines represent the 95% confidence intervals for regression. Correlation was tested with the Pearson r coefficient, while significance is shown with a P value. Data used in the plots are from Tables 2-4. Data are expressed as mean from at least three independent experiments performed in duplicate.

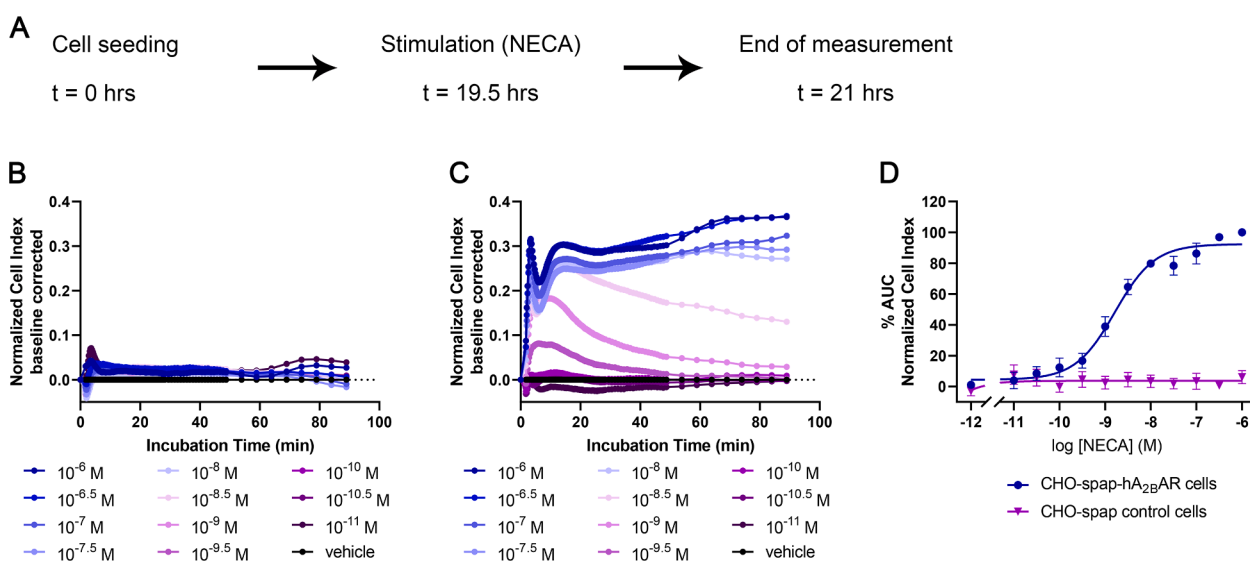


Fig. 4. Functional characterization of NECA on CHO-spap and CHO-spap-hA_{2B}AR cells. (A) Graphic representation of assay set-up. Cell were seeded and 19.5 h later they were stimulated with NECA (10 pM – 1 μ M) and the cell response was monitored for 1.5 h. Representative responses induced by NECA on (B) CHO-spap and (C) CHO-spap-hA_{2B}AR cells. (D) Concentration-response curves of NECA. The curves were normalized to minimum (0%) to maximum response (100%) of CHO-spap-hA_{2B}AR cells. Data shown are mean \pm S.E.M. from at least three separate experiments performed in duplicate.

response measured on CHO-spap-hA_{2B}ARs was only A_{2B}AR mediated, we pre-incubated cells with selective antagonists for each AR subtype prior to NECA stimulation. Only PSB-603, the A_{2B}AR-selective antagonist, inhibited the NECA response, confirming the A_{2B}AR specific hypothesis (Fig. 5A-D). As a result, further experiments for the study of A_{2B}AR were performed on CHO-spap-hA_{2B}AR cells.

After this assay development, chemically similar compounds **17** and **18** but with an 11-fold difference in RT, were selected for further experiments. First, their inhibitory potency in the presence of an EC₈₀ concentration of NECA was determined resulting in pIC₅₀ values of 7.12 ± 0.13 and 6.44 ± 0.21 , respectively (Fig. 6A-D, Table 5). These potencies were found to be approximately 1.5 log unit lower than their affinities determined in the radioligand binding studies (8.64 ± 0.05 and 7.70 ± 0.06 for **17** and **18**, respectively; Table 3), in line with the presence of a high agonist concentration (i.e. EC₈₀) in this assay set-up.

Subsequently, a washout assay was performed and the cell response to the compounds was monitored and evaluated (Fig. 7). In short, cells were pre-treated with a concentration of $30 \times IC_{50}$ of the compounds, and 4 hr later cells were washed, and fresh "serum-free medium" was added (Fig. 7A). For the evaluation of the unwashed condition, the

medium was not refreshed but was pipetted up and down in order to mimic the possible mechanical stress induced to the washed cells. Cells were then stimulated with an EC₈₀ concentration of NECA, enabling us to monitor the response exerted by only those receptors that were not bound to compounds **17** (Fig. 7B) and **18** (Fig. 7C). Based on the experimental set-up, it was hypothesized that the short RT compound was removed more readily during washing, resulting in an increased number of receptors available for NECA to bind and cause a cellular response.

Cells pre-treated with long RT compound **17** showed no significant increase ($p > 0.05$) in NECA signaling after washing (9.8% and 12% for unwashed and washed cells, respectively) (Fig. 7D, Table 5). On the contrary, the increase in NECA signaling between unwashed and washed cells was significantly higher ($P < 0.001$) with the short RT compound **18** (19% and 68% for unwashed and washed cells, respectively) (Fig. 7D, Table 5), verifying our hypothesis. This assay simulates a non-equilibrium condition, not unlike human physiology.

3.2.8. Binding affinity of selected compounds at other adenosine receptors

Selected xanthine derivatives were compared in binding assays [24]

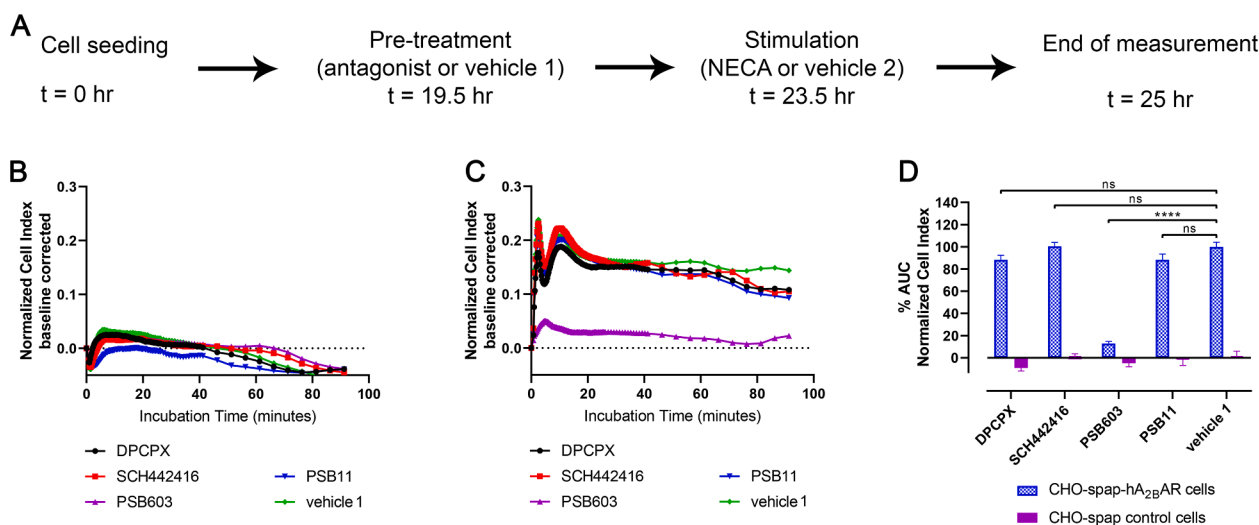


Fig. 5. NECA signaling on CHO-spap and CHO-spap-hA_{2B}AR cells is only mediated via hA_{2B}AR. (A) Graphic representation of assay set-up. Cells were seeded, and 19.5 h later they were pre-treated with an antagonist for all ARs (A₁: DPCPX; A_{2A}: SCH442416; A_{2B}: PSB603; A₃: PSB11). Later they were stimulated with an EC₈₀ concentration of NECA (4 nM) and the cell response was monitored for 1.5 h. Representative responses induced by NECA on (B) CHO-spap and (C) CHO-spap-hA_{2B}AR cells. (D) Bar graphs represent the AUC of antagonists for all ARs after stimulation with EC₈₀ of NECA. The data were normalized to vehicle 1 treated with NECA of CHO-spap-hA_{2B}AR cells as 100%. Data shown are mean ± S.E.M. from at least three separate experiments performed in duplicate. ns *P* > 0.05, **** *P* ≤ 0.001 determined in a one-way ANOVA test with Dunnett's correction.

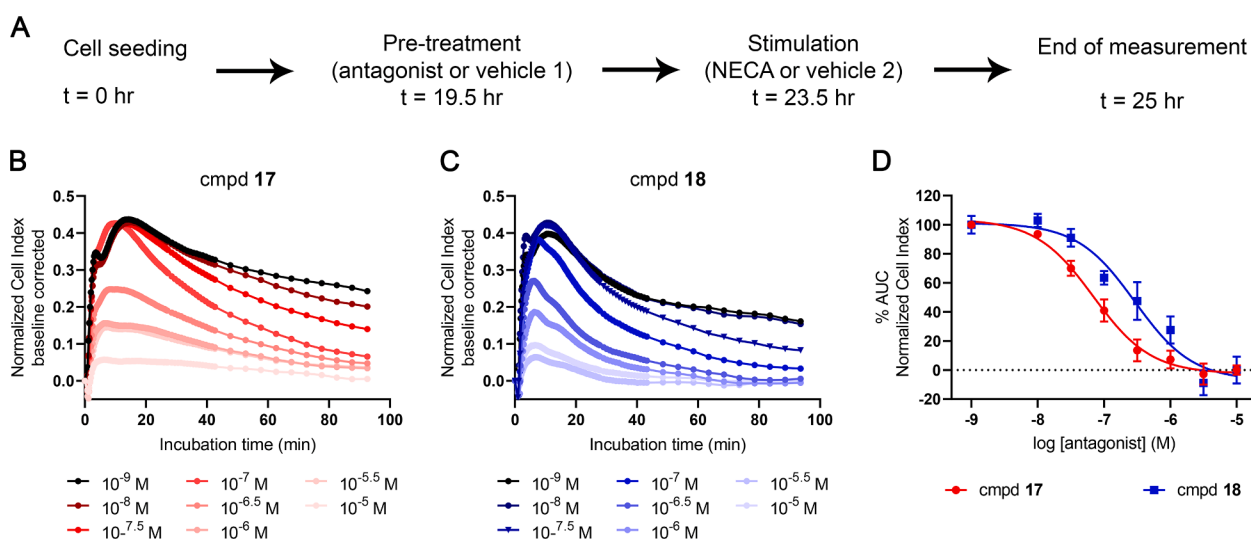


Fig. 6. Functional characterization of compound 17 (short RT) and 18 (long RT) on CHO-spap-hA_{2B}AR cells. (A) Graphic representation of assay set-up. Cells were seeded, and 19.5 hr later they were pre-treated with antagonist 17 or 18 (1 nM – 10 μM) or control (vehicle 1; 0.25% DMSO). After a 4 hr incubation, cells were stimulated with an EC₈₀ concentration of NECA (4 nM) or control (vehicle 2; 0.25% DMSO) and the cell response was monitored for 1.5 hr. (B, C) Representative responses induced by NECA after pre-treatment with various concentrations of compound 17 (B) and compound 18 (C). (D) Concentration-response curves of antagonists after stimulation with EC₈₀ concentration of NECA. The curves were normalized to minimum (0%) and maximum response (100%). Data shown are mean ± S.E.M. from at least three separate experiments performed in duplicate.

at four adenosine receptors (human and rat) as shown in Table 6. The A_{2B} receptor selectivity was generally low, especially at the rat A_{2B} receptor. However, several derivatives, e.g., 20 and 22, displayed mixed higher affinity at the human A_{2B} and A_{2B} receptors compared to the other subtypes.

4. Discussion

Intrigued by earlier studies [34] we combined previously synthesized xanthines with a series of newly synthesized derivatives. In this way we obtained a total of 28 final compounds that were subsequently tested in a variety of assays. The aim was to analyze both their structure-affinity and structure-kinetics relationships, and to test the translational

properties of two selected derivatives in a number of label-free assays. We had performed similar studies on other GPCRs before, and learned that the sole determination of (equilibrium) affinity values provides an incomplete profile of the pharmacological characteristics of receptor ligands. Adding kinetic information informed us better, and made clear that target binding kinetics can dictate the duration of action and the sustainability of a pharmacological effect, thus having an impact on the ligand's pharmacokinetic and pharmacodynamic behavior *in vivo* [35].

We first tested the behavior of [³H]PSB-603, the radioligand used in the present study, and learned that the K_D value we derived was comparable to the value previously reported by Bormann *et al.* [36] A similar K_D value was derived from the kinetic association and dissociation experiments, providing a reliable framework for our further experiments.

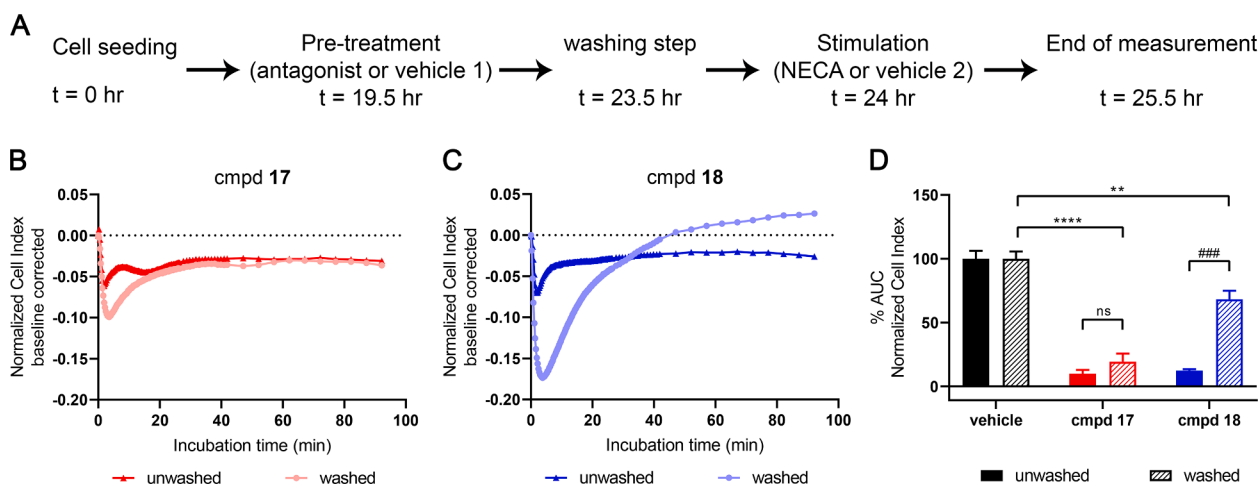


Fig. 7. Recovery of NECA signaling after washing. (A) Graphic representation of assay set-up. Cells were seeded, and 19.5 hr later they were pre-treated with an antagonist ($30 \times IC_{50}$ as determined in the label-free assay in Fig. 6) or control (vehicle 1; 0.25% DMSO). After a 4 hr incubation, cells were washed by removing the medium from the well and replacing it with 95 μ L of fresh serum-free medium. For the unwashed condition, no medium refreshment was done. 30 min afterwards, cells were treated with NECA (at an EC_{80} concentration) or control (vehicle 2; 0.25% DMSO) and the cell response was monitored for 1.5 hr. (B,C) Representative responses induced by NECA with or without washing of cells pre-treated with compound 17 (B) and compound 18 (C). (D) Bar graph showing NECA response after washing step when cells were pre-treated with compound 17 or 18. Bar graphs of both washed and unwashed conditions were compared to the control (vehicle) without any antagonist (100% washed and unwashed AUC, respectively). Data shown are mean \pm S.E.M. from at least three separate experiments performed in duplicate. ns $P > 0.05$, # # # $P \leq 0.001$ determined in an unpaired *t*-test with Welch's correction. ** $P \leq 0.01$, **** $P \leq 0.0001$ determined in a one-way ANOVA test with Dunnett's correction.

Table 6

Comparison of adenosine receptor binding affinities of selected antagonists, expressed as mean \pm S.E.M ($n = 3 - 4$). The species is human, unless noted (r, rat).^a

Compound	K_i (A_1 , nM)	K_i (A_{2A} , nM)	K_i (A_{2B} , nM)	K_i (A_3 , nM)
3	10.7 \pm 1.75 (r)	51.7 \pm 19.6 (r)	36.6 \pm 5.1 (r)	ND
5	13.9 \pm 1.8 (r)	19.1 \pm 5.1 (r)	26.3 \pm 192 (r)	ND
7	23.0 \pm 4.1 (r)	19.3 \pm 6.7 (r)	73.5 \pm 25.8 (r)	ND
19	54.7 \pm 21.2,	23.8 \pm 5.7,	2.04 \pm 0.17,	ND
	5.02 \pm 0.55 (r)	25.9 \pm 7.6 (r)	19.8 \pm 7.9 (r)	ND
20	212 \pm 68,	20.8 \pm 2.4,	8.0 \pm 2.2,	140 \pm 7
	8.85 \pm 1.75 (r)	207 \pm 26 (r)	486 \pm 192 (r)	ND
21	63.9 \pm 16.5,	33.6 \pm 0.1,	5.5 \pm 1.2,	89.9 \pm 11.6
	6.55 \pm 1.27 (r)	251 \pm 33 (r)	20.0 \pm 4.9 (r)	ND
22	586 \pm 250,	26.1 \pm 0.4,	6.8 \pm 0.8	274 \pm 56
	32.7 \pm 1.27 (r)	112 \pm 12 (r)	ND	ND
24	27.3 \pm 4.9,	64.4 \pm 21.2,	8.5 \pm 1.1,	63.9 \pm 16.5
	5.23 \pm 1.13 (r)	375 \pm 139 (r)	21.1 \pm 5.3 (r)	ND
25	23.7 \pm 4.9,	21.0 \pm 1.8,	8.2 \pm 2.5,	156 \pm 15
	10.4 \pm 2.1 (r)	165 \pm 53 (r)	20.2 \pm 4.9 (r)	ND

^a All receptors are expressed in HEK-293 cells. Radioligands used: A_1 , [³H]R-PIA; A_{2A} , [³H]CGS21680; A_{2B} , [¹²⁵I]I-ABOPX; A_3 , [¹²⁵I]I-AB-MECA. ND, not determined.

We then used the radioligand to determine the affinity of the compounds for the hA_{2B}AR. Some of the previously synthesized xanthines had been tested on a number of other human and rat ARs (Table 6), showing a limited selectivity at best. It is important to stress that selectivity was not pursued in the current study.

We then determined the target binding kinetics of the full series of xanthine derivatives following an established protocol by Motulsky and Mahan [32]. This so-called competition association assay has been used to investigate the binding kinetics of ligands for various targets, such as GPCRs [37], kinases [38], transporters [39,40] and other proteins [41]. As the values from the competition association assay were in excellent agreement with the ones from the association and dissociation assay (Table 1), the first was deemed validated for determining an unlabeled ligand's binding kinetics. Evaluation and incorporation of target binding kinetics has been found to be a crucial parameter in drug optimization. The association rate constant is crucial for high target occupancy, due to

the resulting rebinding effect [42], as well as for drug selectivity over different targets and ultimately for increased drug safety [43]. Last but not least, a fast association is crucial for an immediate drug response in case of an acute pathological event [44,45]. As far as the dissociation rate constant is concerned, a slow rate, hence a long RT is required for a longer and/or a more durable, sustained effect [46]. If RT exceeds the pharmacokinetic half-life, the drug could maintain its effect even past plasma clearance, resulting in potential advantages like a decreased frequency of drug dosing and a reduction in off-target toxic effects [43,47]. The compounds showed largely varying equilibrium affinity values as well as kinetic rate constants and corresponding residence times (RTs). Among the compounds was the prototypic A_{2B}AR antagonist MRS1754 (13). In the displacement assay an affinity of 1.78 nM was determined for 13, which was in excellent agreement with data reported by Ji *et al.* [48]. The kinetic characterization of 13, yielding an RT of 69 min, made us increase the duration of the competition association assay from an initial 45 min to 3 h in order to allow for the longer RT compounds to reach equilibrium. As a result the 3 hr incubation assay was used for the determination of kinetic binding parameters for all qualifying A_{2B}AR antagonists. Compound 3 had the shortest RT (0.9 min), while compound 17 was endowed with the longest (87 min). Overall, there was a significant correlation between affinity and dissociation rate constants of all compounds for which we were able to obtain the kinetic parameters (Fig. 3C).

Due to its high chemical similarity we chose compound 18 (RT = 8.0 min) as a benchmark comparator for compound 17. We performed radioligand washout experiments with both compounds and compared their behavior with that of a putatively covalent antagonist (29). It appeared that 18 was rapidly dissociating from the receptor under washing conditions, while 17 was much more resistant, although less so than 29. Currently, A_{2B}AR antagonists are in clinical stages of testing for their immuno-oncological behavior (*vide supra* and ref [14]). The tumor micro-environment where the compounds supposedly act is under the influence of high adenosine levels. Hence antagonists with longer RT, counterbalancing this adenosine "pressure", may be very useful.

Next to binding parameters we studied compounds 17 and 18 in a functional set-up, in order to investigate the link between binding kinetics and a possibly prolonged functional effect. For this purpose a so-

called label-free assay was developed with xCELLigence technology, measuring changes in cellular impedance that are expressed as a unitless parameter named Cell Index [28,30]. As mentioned before we found a relatively high potency [49,50] for the reference, non-selective, AR agonist NECA, although it complies with other data in literature [51–54]. Hence, we made sure that the effects seen were entirely due to interactions with the A_{2B}AR. The same assay was used to study wash-out of the two compounds, simulating a non-equilibrium condition not unlike human physiology. As a result, findings from this assay, with 17 largely maintaining its effect, constitute a possible translational step towards *in vivo* experiments [27,55].

In conclusion we reported the synthesis and pharmacological evaluation of a series of xanthine-based analogues designed as hA_{2B}AR antagonists. A radioligand competition association assay was developed to evaluate kinetic binding parameters next to affinity. Structure-affinity and structure-kinetic relationships (SAR and SKR) were examined and a great spread in target residence time (RT) was observed, from 0.9 min (3) to 87 min (17). Based on correlation plots, the dissociation rate constant appeared the driving force for affinity unlike the association rate constants. Subsequently two compounds (17 and 18) with long and short RT, respectively, were selected and tested in a label-free impedance-based assay. These experiments confirmed the link between long RT and an extended pharmacological effect under non-equilibrium conditions. To our knowledge, this is the first SKR study performed on hA_{2B}AR antagonists, which could pave the way to the development of clinically meaningful antagonists, e.g., in immune-oncology, with a high affinity and long residence time at the A_{2B}AR.

Declaration of Competing Interest

The authors declare that they have no known competing financial interests or personal relationships that could have appeared to influence the work reported in this paper.

Acknowledgements

KAJ acknowledges support from the NIDDK Intramural Research Program, United States (ZIADK031117).

References

- M.A. Jacobson, R.G. Johnson, C.J. Luneau, C.A. Salvatore, Cloning and chromosomal localization of the human A_{2B} adenosine receptor gene (ADORA2B) and its pseudogene, *Genomics* 27 (2) (1995) 374–376.
- B.B. Fredholm, A.P. IJzerman, K.A. Jacobson, K.-N. Klotz, J. Linden, International Union of Pharmacology. XXV. Nomenclature and Classification of Adenosine Receptors, *Pharmacol. Rev.* 53(4) (2001) 527–552.
- S. Gessi, K. Varani, S. Merighi, E. Leung, S. Mac Lennan, P.G. Baraldi, P.A. Borea, Novel selective antagonist radioligands for the pharmacological study of A_{2B} adenosine receptors, *Purinergic Signalling* 2 (4) (2006) 583–588.
- M.W. Beukers, H. den Dulk, E.W. van Tilburg, J. Brouwer, A.P. IJzerman, Why Are A_{2B} Receptors Low-Affinity Adenosine Receptors? Mutation of Asn273 to Tyr Increases Affinity of Human A_{2B} Receptor for 2-(1-Hexynyl)adenosine, *Mol. Pharmacol.* 58(6) (2000) 1349–1356.
- B.B. Fredholm, A.P. IJzerman, K.A. Jacobson, J. Linden, C.E. Müller, International Union of Basic and Clinical Pharmacology. LXXXI. Nomenclature and Classification of Adenosine Receptors—An Update, *Pharmacol. Rev.* 63 (1) (2011) 1–34.
- I. Feoktistov, I. Biaggioni, Adenosine A_{2B} receptors, *Pharmacol. Rev.* 49 (4) (1997) 381–402.
- Y. Zhou, D.J. Schneider, M.R. Blackburn, Adenosine signaling and the regulation of chronic lung disease, *Pharmacol. Ther.* 123 (1) (2009) 105–116.
- L. Spicuzza, G. Di Maria, R. Polosa, Adenosine in the airways: implications and applications, *Eur. J. Pharmacol.* 533 (1–3) (2006) 77–88.
- V.L. Kolachala, M. Vijay-Kumar, G. Dalmasso, D. Yang, J. Linden, L. Wang, A. Gewirtz, K. Ravid, D. Merlin, S.V. Sitaraman, A_{2B} adenosine receptor gene deletion attenuates murine colitis, *Gastroenterology* 135 (3) (2008) 861–870.
- A. El-Tayeb, S. Michael, A. Abdelrahman, A. Behrenswerth, S. Gollos, K. Nieber, C. E. Müller, Development of Polar Adenosine A_{2A} Receptor Agonists for Inflammatory Bowel Disease: Synergism with A_{2B} Antagonists, *ACS Med. Chem. Lett.* 2 (12) (2011) 890–895.
- H. Harada, O. Asano, Y. Hoshino, S. Yoshikawa, M. Matsukura, Y. Kabasawa, J. Nijijima, Y. Kotake, N. Watanabe, T. Kawata, T. Inoue, T. Horioze, N. Yasuda, H. Minami, K. Nagata, M. Murakami, J. Nagaoka, S. Kobayashi, I. Tanaka, S. Abe, 2-Alkynyl-8-aryl-9-methyladenines as novel adenosine receptor antagonists: their synthesis and structure-activity relationships toward hepatic glucose production induced via agonism of the A(2B) receptor, *J. Med. Chem.* 44 (2) (2001) 170–179.
- Z. Wei, S. Costanzi, R. Balasubramanian, Z.-G. Gao, K.A. Jacobson, A_{2B} adenosine receptor blockade inhibits growth of prostate cancer cells, *Purinergic Signalling* 9 (2) (2013) 271–280.
- S. Viganò, D. Alatzoglou, M. Irving, C. Menetrier-Caux, C. Caux, P. Romero, G. Coukos, Targeting Adenosine in Cancer Immunotherapy to Enhance T-Cell Function, *Front Immunol* 10 (2019) 925.
- Z.-G. Gao, K.A. Jacobson, A_{2B} Adenosine Receptor and Cancer, *Int. J. Mol. Sci.* 20 (2019) 5139.
- R.V. Kalla, J. Zablocki, Progress in the discovery of selective, high affinity A(2B) adenosine receptor antagonists as clinical candidates, *Purinergic Signalling* 5 (1) (2009) 21–29.
- M. Lindemann, S. Dukic-Stefanovic, S. Hinz, W. Deuther-Conrad, R. Teodoro, C. Juhl, J. Steinbach, P. Brust, C.E. Müller, B. Wenzel, Synthesis of Novel Fluorinated Xanthine Derivatives with High Adenosine A(2B) Receptor Binding Affinity, *Pharmaceuticals (Basel)* 14 (5) (2021) 485, <https://doi.org/10.3390/ph14050485>.
- M. Majellaro, W. Jespers, A. Crespo, M.J. Núñez, S. Novio, J. Azuaje, R. Prieto-Díaz, C. Gioè, B. Alispahic, J. Brea, M.I. Loza, M. Freire-Garabal, C. Garcia-Santiago, C. Rodríguez-García, X. García-Mera, O. Caamaño, C. Fernandez-Masaguer, J.F. Sardina, A. Stefanachi, A. El Maatougui, A. Mallo-Abreu, J. Àqvist, H. Gutiérrez-de-Terán, E. Sotelo, 3,4-Dihydropyrimidin-2(1H)-ones as Antagonists of the Human A(2B) Adenosine Receptor: Optimization, Structure-Activity Relationship Studies, and Enantiospecific Recognition, *J. Med. Chem.* 64 (1) (2021) 458–480.
- A. Mallo-Abreu, R. Prieto-Díaz, W. Jespers, J. Azuaje, M. Majellaro, C. Velando, X. García-Mera, O. Caamaño, J. Brea, M.I. Loza, H. Gutiérrez-de-Terán, E. Sotelo, Nitrogen-Walk Approach to Explore Bioisosteric Replacements in a Series of Potent A(2B) Adenosine Receptor Antagonists, *J. Med. Chem.* 63 (14) (2020) 7721–7739.
- C.E. Müller, Y. Baqi, S. Hinz, V. Namasivayam, Medicinal Chemistry of A_{2B} Adenosine Receptors, in: P.A. Borea, K. Varani, S. Gessi, S. Merighi, F. Vincenzi (Eds.), *The Adenosine Receptors*, Springer International Publishing, Cham, 2018, pp. 137–168, https://doi.org/10.1007/978-3-319-90808-3_6.
- Clinical Trials, PBF-1129 in Patients With NSCLC. (Accessed Accessed on 13-Jan-2022, <https://clinicaltrials.gov/ct2/show/NCT03274479?term=ADORA2B&dr aw=2&rank=1>).
- F.F. Sherbiny, A.C. Schiedel, A. Maass, C.E. Müller, Homology modelling of the human adenosine A_{2B} receptor based on X-ray structures of bovine rhodopsin, the beta₂-adrenergic receptor and the human adenosine A_{2A} receptor, *J. Comput. Aided Mol. Des.* 23 (11) (2009) 807–828.
- D.C. Swinney, B.A. Haubrich, I. Van Liefde, G. Vauquelin, The Role of Binding Kinetics in GPCR Drug Discovery, *Curr. Top. Med. Chem.* 15 (24) (2015) 2504–2522.
- E. Lindström, B. von Mentzer, I. Pählman, I. Ahlstedt, A. Uvebrant, E. Kristensson, R. Martinsson, A. Novén, J. de Verdier, G. Vauquelin, Neurokinin 1 Receptor Antagonists: Correlation between *In Vitro* Receptor Interaction and *In Vivo* Efficacy, *J. Pharmacol. Exp. Ther.* 322 (3) (2007) 1286–1293.
- Y.-C. Kim, X.-D. Ji, N. Melman, J. Linden, K.A. Jacobson, Anilide Derivatives of an 8-Phenylxanthine Carboxylic Congener Are Highly Potent and Selective Antagonists at Human A_{2B} Adenosine Receptors, *J. Med. Chem.* 43 (6) (2000) 1165–1172.
- K.A. Jacobson, K.L. Kirk, W.L. Padgett, J.W. Daly, Functionalized congeners of 1,3-dialkylxanthines: preparation of analogs with high affinity for adenosine receptors, *J. Med. Chem.* 28 (9) (1985) 1334–1340.
- P.K. Smith, R.I. Krohn, G.T. Hermanson, A.K. Mallia, F.H. Gartner, M. D. Provenzano, E.K. Fujimoto, N.M. Goeke, B.J. Olson, D.C. Klenk, Measurement of protein using bicinchoninic acid, *Anal. Biochem.* 150 (1) (1985) 76–85.
- B. Xi, N. Yu, X. Wang, X. Xu, Y. Abassi, The application of cell-based label-free technology in drug discovery, *Biotechnol. J.* 3 (4) (2008) 484–495.
- N. Yu, J.M. Atienza, J. Bernard, S. Blanc, J. Zhu, X. Wang, X. Xu, Y.A. Abassi, Real-Time Monitoring of Morphological Changes in Living Cells by Electronic Cell Sensor Arrays: An Approach To Study G Protein-Coupled Receptors, *Anal. Chem.* 78 (1) (2006) 35–43.
- J.M. Hillger, J. Schoop, D.I. Boomsma, P. Eline Slagboom, A.P. IJzerman, L. H. Heitman, Whole-cell biosensor for label-free detection of GPCR-mediated drug responses in personal cell lines, *Biosens. Bioelectron.* 74 (2015) 233–242.
- Y.e. Fang, The development of label-free cellular assays for drug discovery, *Expert Opin. Drug Discov.* 6 (12) (2011) 1285–1298.
- C. Yung-Chi, W.H. Prusoff, Relationship between the inhibition constant (KI) and the concentration of inhibitor which causes 50 per cent inhibition (I50) of an enzymatic reaction, *Biochem. Pharmacol.* 22 (23) (1973) 3099–3108.
- H.J. Motulsky, L.C. Mahan, The kinetics of competitive radioligand binding predicted by the law of mass action, *Mol. Pharmacol.* 25 (1) (1984) 1–9.
- R.A. Copeland, Evaluation of enzyme inhibitors in drug discovery. A guide for medicinal chemists and pharmacologists, *Methods Biochem. Anal.* 46 (2005) 1–265.
- J. Zablocki, E. Elzein, R. Kalla, A_{2B} adenosine receptor antagonists and their potential indications, *Expert Opin. Ther. Pat.* 16 (10) (2006) 1347–1357.
- D. Guo, J.M. Hillger, A.P. IJzerman, L.H. Heitman, Drug-target residence time—a case for G protein-coupled receptors, *Med. Res. Rev.* 34 (4) (2014) 856–892.
- T. Borrmann, S. Hinz, D.C.G. Bertarelli, W. Li, N.C. Florin, A.B. Scheiff, C.E. Müller, 1-Alkyl-8-(piperazine-1-sulfonyl)phenylxanthines: Development and Characterization of Adenosine A_{2B} Receptor Antagonists and a New Radioligand

- with Subnanomolar Affinity and Subtype Specificity, *J. Med. Chem.* 52 (13) (2009) 3994–4006.
- [37] D.A. Sykes, L.A. Stoddart, L.E. Kilpatrick, S.J. Hill, Binding kinetics of ligands acting at GPCRs, *Mol. Cell. Endocrinol.* 485 (2019) 9–19.
- [38] J.M. Bradshaw, J.M. McFarland, V.O. Paavilainen, A. Biscante, D. Tam, V.T. Phan, S. Romanov, D. Finkle, J. Shu, V. Patel, T. Ton, X. Li, D.G. Loughhead, P.A. Nunn, D.E. Karr, M.E. Gerritsen, J.O. Funk, T.D. Owens, E. Verner, K.A. Brameld, R.J. Hill, D.M. Goldstein, J. Taunton, Prolonged and tunable residence time using reversible covalent kinase inhibitors, *Nat. Chem. Biol.* 11 (7) (2015) 525–531.
- [39] P.R. Tsuruda, J. Yung, W.J. Martin, R. Chang, N. Mai, J.A.M. Smith, Influence of ligand binding kinetics on functional inhibition of human recombinant serotonin and norepinephrine transporters, *J. Pharmacol. Toxicol. Methods* 61 (2) (2010) 192–204.
- [40] A. Vlachodimou, K. Konstantinopoulou, A.P. IJzerman, L.H. Heitman, Affinity, binding kinetics and functional characterization of draflazine analogues for human equilibrative nucleoside transporter 1 (SLC29A1), *Biochem. Pharmacol.* 172 (2020) 113747.
- [41] B. Costa, E. Da Pozzo, C. Giacomelli, E. Barresi, S. Taliani, F. Da Settimo, C. Martini, TSPO ligand residence time: a new parameter to predict compound neurosteroidogenic efficacy, *Sci. Rep.* 6 (2016) 18164.
- [42] W.E.A. de Witte, M. Danhof, P.H. van der Graaf, E.C.M. de Lange, In vivo target residence time and kinetic selectivity: The association rate constant as determinant, *Trends Pharmacol. Sci.* 37 (10) (2016) 831–842.
- [43] P.J. Tonge, Drug-Target Kinetics in Drug Discovery, *ACS Chem. Neurosci.* 9 (1) (2018) 29–39.
- [44] G.F. Smith, Medicinal Chemistry by the Numbers: The Physicochemistry, Thermodynamics and Kinetics of Modern Drug Design, in: G. Lawton, D.R. Witty (Eds.), *Progress in Medicinal Chemistry*, Elsevier, 2009, pp. 1–29.
- [45] A.P. IJzerman, D. Guo, Drug-Target Association Kinetics in Drug Discovery, *Trends Biochem. Sci.* 44 (10) (2019) 861–871.
- [46] P.J. Tummino, R.A. Copeland, Residence Time of Receptor–Ligand Complexes and Its Effect on Biological Function, *Biochemistry* 47 (20) (2008) 5481–5492.
- [47] R.A. Copeland, The drug-target residence time model: a 10-year retrospective, *Nat. Rev. Drug Discov.* 15 (2) (2016) 87–95.
- [48] X.-D. Ji, Y.-C. Kim, D.G. Ahern, J. Linden, K.A. Jacobson, [3H]MRS 1754, a selective antagonist radioligand for A(2B) adenosine receptors, *Biochem. Pharmacol.* 61 (6) (2001) 657–663.
- [49] M. de Zwart, R. Link, J.K. von Frijtag Drabbe Kunzel, G. Cristalli, K.A. Jacobson, A. Townsend-Nicholson, A.P. IJzerman, A functional screening of adenosine analogues at the adenosine A2B receptor: a search for potent agonists, *Nucleosides Nucleotides* 17 (6) (1998) 969–985.
- [50] M. de Lera Ruiz, Y.-H. Lim, J. Zheng, Adenosine A2A Receptor as a Drug Discovery Target, *J. Med. Chem.* 57 (9) (2014) 3623–3650.
- [51] D. Beattie, A. Brearley, Z. Brown, S.J. Charlton, B. Cox, R.A. Fairhurst, J.R. Fozard, P. Gedeck, P. Kirkham, K. Meja, L. Nanson, J. Neef, H. Oakman, G. Spooner, R. J. Taylor, R.J. Turner, R. West, H. Woodward, Synthesis and evaluation of two series of 4'-aza-carbocyclic nucleosides as adenosine A2A receptor agonists, *Bioorg. Med. Chem. Lett.* 20 (3) (2010) 1219–1224.
- [52] L. Aurelio, J.-A. Baltos, L. Ford, A.T.N. Nguyen, M. Jörg, S.M. Devine, C. Valant, P. J. White, A. Christopoulos, L.T. May, P.J. Scammells, A Structure-Activity Relationship Study of Bitopic N6-Substituted Adenosine Derivatives as Biased Adenosine A1 Receptor Agonists, *J. Med. Chem.* 61 (5) (2018) 2087–2103.
- [53] S.M. Devine, L.T. May, P.J. Scammells, Design, synthesis and evaluation of N6-substituted 2-aminoadenosine-5'-N-methylcarboxamides as A3 adenosine receptor agonists, *MedChemComm* 5 (2) (2014) 192–196.
- [54] G. Schulte, B.B. Fredholm, Human adenosine A(1), A(2A), A(2B), and A(3) receptors expressed in Chinese hamster ovary cells all mediate the phosphorylation of extracellular-regulated kinase 1/2, *Mol. Pharmacol.* 58 (3) (2000) 477–482.
- [55] M.L.J. Doornbos, J.M. Cid, J. Haubrich, A. Nunes, J.W. van de Sande, S.C. Vermond, T. Mulder-Krieger, A.A. Trabanco, A. Ahnaou, W.H. Drinkenburg, H. Lavreysen, L.H. Heitman, A.P. IJzerman, G. Tresadern, Discovery and kinetic profiling of 7-Aryl-1,2,4-triazolo[4,3-a]pyridines: positive allosteric modulators of the metabotropic glutamate receptor 2, *J. Med. Chem.* 60(15) (2017) 6704–6720.